# EVALUATING PERMEABILITY ANISOTROPY IN THE EARLY JURASSIC TILJE FORMATION, OFFSHORE MID-NORWAY

A Thesis

by

KANAN R. ALIYEV

Submitted to the Office of Graduate Studies of
Texas A&M University
in partial fulfillment of the requirements for the degree of

MASTER OF SCIENCE

August 2004

Major Subject: Petroleum Engineering

**EVALUATING PERMEABILITY ANISOTROPY IN THE EARLY JURASSIC TILJE FORMATION, OFFSHORE MID-NORWAY**

A Thesis

by

KANAN R. ALIYEV

Submitted to Texas A&M University
in partial fulfillment of the requirements
for the degree of

MASTER OF SCIENCE

Approved as to style and content by:

| | |
|---|---|
| Jerry L. Jensen<br>(Co-Chair of Committee) | Brian Willis<br>(Co-Chair of Committee) |
| Bryan Maggard<br>(Member) | Stephen Holditch<br>(Head of Department) |

August 2004

Major Subject: Petroleum Engineering

# ABSTRACT

Evaluating Permeability Anisotropy in the Early Jurassic
Tilje Formation, Offshore Mid-Norway. (August 2004)
Kanan R. Aliyev, B.S., Baku State University, Azerbaijan;
M.S., Baku State University, Azerbaijan
Co-Chairs of Advisory Committee: Dr. Jerry L. Jensen
Dr. Brian Willis

The problem of evaluating permeability anisotropy in the Tilje Formation, Heidrum field, offshore mid-Norway, has been investigated by the Statoil Research Centre by a detailed combination of the geological and petrophysical data.

The large diversity and contrasting levels of heterogeneity within depositional facies observed in the Tilje Formation reflect complicated patterns of deposition along deltaic shorelines and the adjunct shelf of a tidally influenced, narrow seaway. Permeability anisotropy can alter the directionality of the fluid flow in the reservoir, and thereby affect the most important exploration procedures: perforation, water and gas injection, production, and estimation of the field resource.

This thesis presents a simplified method of modeling permeability anisotropy in the Tilje Formation.

## DEDICATION

This thesis is dedicated:

*To the glory of Allah*

*To my parents, Rasim and Malakhat*

*To my sister and brother, Vafa and Ayaz*

*To my fiancé, Parvina*

## ACKNOWLEDGMENTS

I would like to express my sincere gratitude and appreciation to Dr. Jerry L. Jensen, the co-chair of my advisory committee, for his assistance, encouragement, guidance, and constructive remarks throughout this research. Thanks to his vision and experience, which motivated me to the completion of this work.

Also, I would like to acknowledge Dr. Brian Willis for serving as my co-chair and Dr. Bryan Maggard for servicing as a member of the advisory committee. Thanks to both for their support and creative approach to resolving my research problems.

I also express my thankfulness to all of my friends, whom I met here and whom I left back home, for their valuable support, encouragement, advice, and help in difficult times.

# TABLE OF CONTENTS

CHAPTER Page

## LIST OF FIGURES

FIGURE Page

# LIST OF TABLES

# CHAPTER I
# INTRODUCTION

## 1.1 Permeability anisotropy

*Anisotropy,* the directional variation of a reservoir, occurs in flow or transport variables like permeability, resistivity, and thermal conductivity. Permeability anisotropy can cause a change of flow direction (Figure 1-1). Permeability anisotropy may be related to depositional processes that formed the reservoir rock and the resulting spatial variations in lithic properties. Depositional environment controls the composition and geometry of lithologic variations (Lake, 1988).

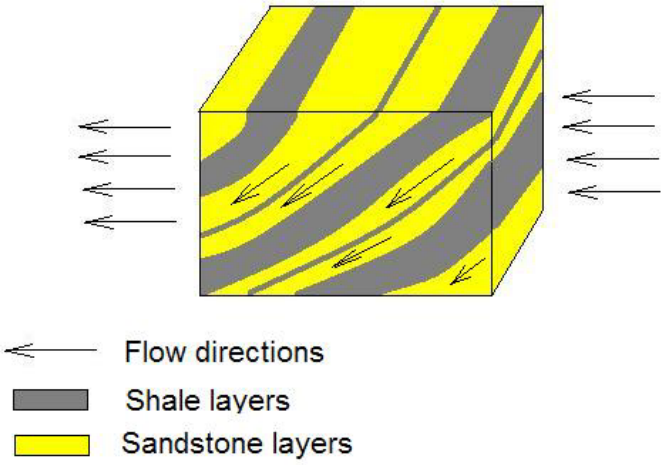


**Figure 1-1.** Reservoir flow is changed by contrast between horizontal and vertical permeability

Anisotropy is scale dependant. Core plug anisotropy and whole-core anisotropy often differ because the core plug measurement is supported by a smaller volume of rock. Permeability measurements can also differ with change in the direction and size of the core plug relative to the orientation of the internal lithic changes (Willhite, 1986, Figure 1-2). Even where individual sandstone and shale layers are internally isotropic,

This thesis follows the style and format of the AAPG Bulletin.

variations between layers can produce large-scale field anisotropy. Permeability anisotropy commonly increases when increasing rock volumes are examined, reflecting large-scale sedimentlogical structures and lithofacies within the formation (Jensen *et al.*, 2003).

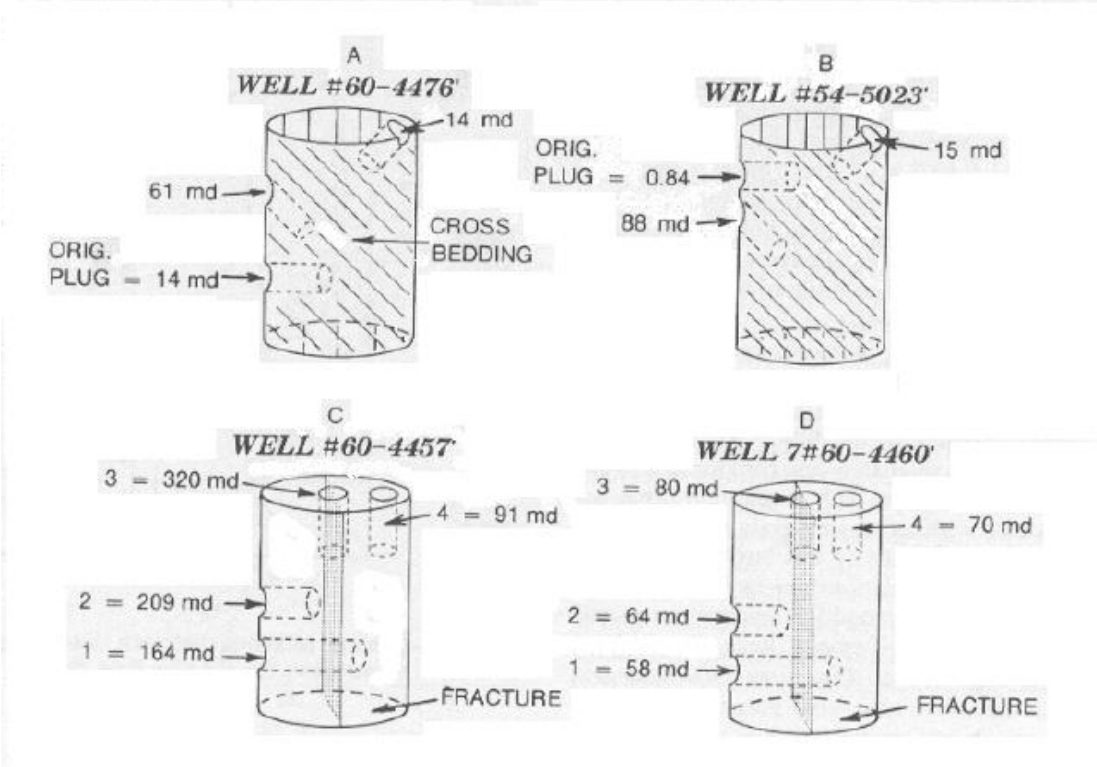


**Figure 1-2**. Size and direction of core plug sample affects permeability values

Permeability anisotropy can alter the direction of fluid flow through the reservoir, which in turn affects the performance of perforations, water and gas injection, production behavior, and estimates of the field resource. Field case-study, (e.g., Cowan and Bradney, 1997) permeability anisotropy effects are presented in Chapter II.

### 1.2 Description of study problem

Effects of permeability anisotropy within the reservoir of the Tilje Formation, Heidrun Field, offshore mid-Norway, have been investigated by Statoil Research Center

by combining geological and petrophysical data in reservoir simulation models (Martinius *et al.,* 1999). Their evaluation methods were elaborate and expensive, including a large nomber of geologists and engineers working over a period of years. This project presents a simpler method of modeling permeability anisotropy in the Tilje Formation, which may be appropriate for the evaluation of less economically valuable reservoirs. The results of this simpler evaluation will be compared with those of the more elaborate the models used by Statoil Research Center.

Martinius *et al.* (1999) carried out an experiment of multiscale characterization and modeling of $k_v/k_h$ ($k_v$ is vertical permeability; $k_h$ horizontal permeability) in Heidrun Field. They used a combination of statistical, object-based, sedimentary models to predict the geometry of lithologic volumes in different parts of the field and of rock properties from cores of the reservoir to derive field-scale reservoir properties. Three-dimensional heterogeneity within facies associations was modeled using type-curves that related the horizontal and vertical permeability to functions of observed net-to-gross ratio, bed thickness, and permeability of sand and shale layers. Permeability and anisotropy of different types of rock units varied significantly, and multiple realizations of geostatistical models of reservoir architecture predicted a wide range of possible reservoir-prediction behavior.

The large diversity and contrasting levels of heterogeneity within depositional facies observed in the Tilje Formation reflect complicated patterns of deposition along deltaic shorelines and the adjunct shelf of a tidally influenced, narrow seaway. Martinius *et al.* (1999) concluded that the permeability ratio ($k_v/k_h$) is the most critical parameter controlling reservoir production behavior and confirmed the significant influence of depositional heterogeneity on patterns of reservoir flow.

Lithofacies exhibit various degrees of internal heterogeneity, depending on the degrees of variation in grain size and sorting across sedimentary structures and beds, and the extent of cementation. This study evaluates facies imposition factors that affect permeability anisotropy. Geostatistical, geological, and well-log analysis used in this evaluation were limited somewhat by the available data.

# CHAPTER II
# LITERATURE REVIEW

## 2.1 Scale of permeability anisotropy

Methods used to evaluate permeability anisotropy include core analysis, well testing, tidal-pressure monitoring, wireline-formation testers, and probe minipermeameter measurements of the core plugs. Ayan *et al.* (1994) investigated permeability anisotropy using a formation tester (Figure 2-1). Pressure fluctuations during the tests depend on the vertical and horizontal permeability and reservoir boundaries. A Modular Formation Dynamic Tester (MDT) allows evaluation of permeability anisotropy in openhole conditions and at partially perforated intervals. Three flow patterns are measured during a test: early radial flow, and successive later spherical and global radial flow (Figure 2a). Patterns of flow for openhole and partially perforated cases differ (Figure 2b, c).

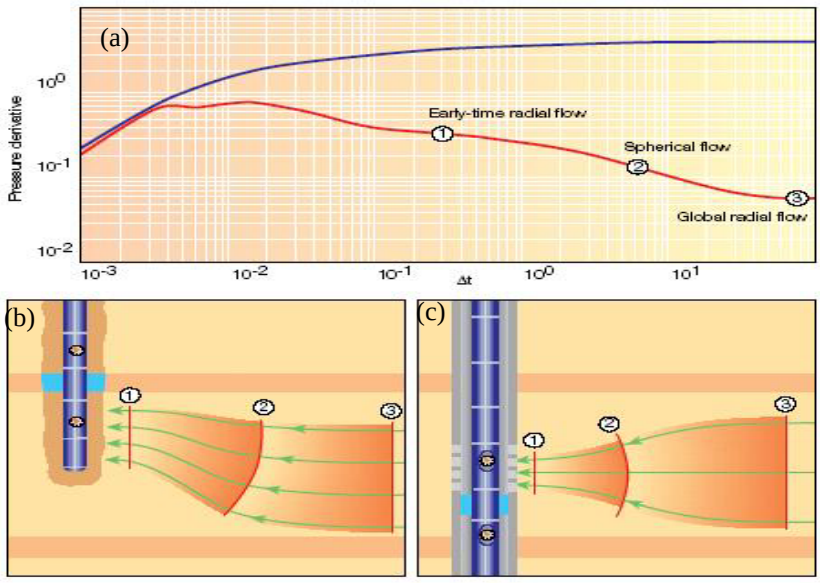


**Figure 2-1.** Permeability anisotropy observed during formation-tester analysis (from Oilfield Review, 1994)

Horizontal permeability can be calculated assuming a radial flow pattern early in the test. Spherical flow, assumed to occur later in the test, can be used to calculate the geometric mean of horizontal ($k_h$) and vertical ($k_v$) permeability. From comparing of these two calculations, vertical permeability can be estimated. This method allows an assessment of the effect of laterally extensive, low-permeability layers on reservoir flow patterns.

Static and dynamic measurements of permeability anisotropy can vary with the scale of the measurement (Morton *et al.,* 2002). Morton *et al.,* compared permeability estimates from core plugs, minipermeameter-probe measurements, Interval Pressure Transient Tests (IPTT), and borehole images. Formation tests measure permeability at bed to bedsets scales (meters to tens of meters), whereas core plug and probe minipermeameters measure small scales. Because these estimates are based on different methods, variation of results cannot be related to scale alone. Core-permeability data were collected under laboratory conditions at atmospheric pressure, whereas formation tests are conducted at *in-situ* conditions under reservoir pressures and temperatures. Clay -bound water can affect the predictions of permeability from borehole electrical images, generally overestimating vertical permeability through high clay intervals. The comparison by Morton *et al*. (2002) indicated that core plug and probe-scale permeability do not capture permeability anisotropy because of these different scales heterogeneity within the reservoir rock.

**2.2 Anisotropic effect on horizontal wells**

Decreased permeability ratio ($k_v/k_h$) reduces deliverability of a horizontal well in turn reducing the economics of such wells (Figure 2-2).

Developments in drilling technology have allowed more wells to be deviated to horizontal at depth. A horizontal wellbore contacts a relatively large reservoir area, which can more effectively drain hydrocarbons or spread injected fluids for pressure maintenance.

Cowan and Bradney (1997) discuss effects of permeability anisotropy created by cemented zones on the ability of horizontal wells to effectively drain a gas reservoir in the Millom accumulation. To explore a gas reservoir efficiently, they proposed the drilling of the vertical wells.

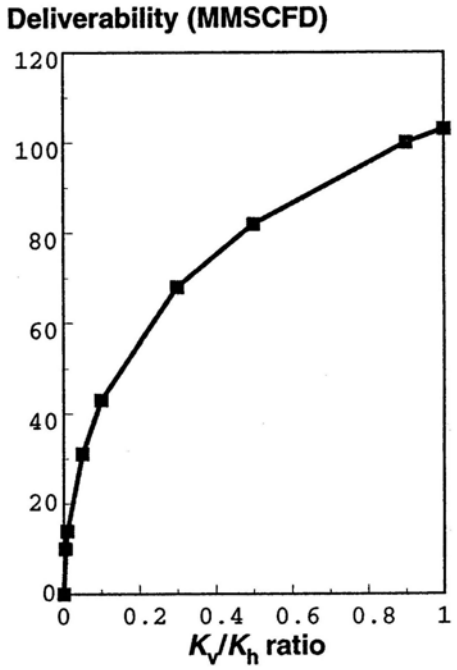


**Figure 2-2.** Horizontal well deliverability as a function of permeability ratio

Exploration in the Millom accumulation is complicated by the geologic architecture of the reservoir. Hydrocarbon accumulated in thin sandstone layers with good reservoir properties between layers of the platy illite, quartz, and carbonate cementation (Cowan and Bradney, 1997). Several analyses, such as probe minipermeametry, core plug, Modular Formation Dynamic Tester (MDT) and tidal pressure analyses were conducted at different scale to evaluate the permeability anisotropy. The results of analysis suggest the insufficiency of the horizontal wells to develop the reservoir.

## 2.3 Anisotropy caused by shale

Permeability anisotropy depends on the lateral extent of shale beds and shale-bed composition. Effective permeability can be estimated using 3D reservoir models that predict properties of small, discontinues barriers imbedded within more permeable simulation gridblocks. To generate the shale barriers within the gridblock, a stochastic approach is used.

Kasap (2001) presented three models to assess the permeability anisotropy, simulating the path of flow through conductive and nonconductive layers. The models estimate the permeability anisotropy produced by shale with realistic geometry and various length, width, and thickness distributions. The main purpose of these techniques is to evaluate permeability when the flow bypasses or goes through the small-scale shale layers. To accommodate limitations of mathematical simulations, he assumed that flow is perpendicular to the barrier and once reflected goes back to its origin. This approach requires an exactly known shale distribution within simulation blocks, whether it is deterministic or stochastic.

Effects of the dimension, thickness, and fraction of shale layers on vertical permeability were investigated by Begg and King (1985). They investigated four methods - analytical, statistical, simulation and streamline - to assess effective vertical permeability with different parameters for 2D and 3D models. They assumed unidirectional, steady-state flow of a single, incompressible fluid. Because computing time was a constraint, they used only one grid. Assumed that shale layers within the simulation gridblock had the same direction and orientation, Begg and King (1985) calculated the flow around the impermeable layers. Elliptical and spheroidal coordinates were used to represent shale layers as line segments and disc of radius, respectively. Although this approach was similar to that used by Kasap (2001), he assumed a rectangular shape of the surface of shale layers. Begg and King (1985) found good agreement between results from analytical, explicit streamline, and simulation of 2D and 3D models. Although the effect of the boundary conditions is observed in statistical

models, the difference was not significant. The shale dimension and thickness strongly influence the results of experiments.

Peffer *et al.* (1997) used formation-tester experiments to determine the vertical distribution permeability anisotropy in the Triassic Argileux Greseux Interferiur (TAGI). Four sandstone sections with small shale intervals were chosen on the basis of core description and well-log information. Single- and multiple-layer interpretations were conducted to investigate *in-situ* permeability anisotropy. Interpretations of shale distributions were judged by matching with core analysis. Lithic variations observed in the core were compared with formation-tester measurements. In general, agreement between core-derived and formation-tester-determined permeability anisotropies is good (Peffer *et al.*, 1997), which supports the use of the openhole, packer-probe formation tester to measure *in-situ* permeability anisotropy.

Core plug and minipermeameter permeability data can be used to evaluate permeability anisotropy of reservoir rocks. Minipermeameter measurements can capture mm-scale sedimentary layering. Hurst and Rosvell (1991) collected more than 16,000 probe data from cored sandstones of the Fangst and Bat groups, Norwegian continental shelf. Comprehensive analyses were conducted to evaluate the permeability of large-scale and small-scale horizontal stratification and of massive and heterolithic sandstones. The density of the minipermeametry sampling changes average permeability estimates, even for the most homogeneous rocks. Averages of probe-permeability measurements were similar to whole-core permeability measurements.

**2.4 Comparative analysis**

With the increased role of reservoir characterization in reservoir modeling, applied statistics summarizing rock properties are becoming increasingly important. Statistics estimate the distribution of reservoir properties: permeability, porosity, and capillary pressure. A variety of the statistical tools is used to assess these distributions and to quantify the differences.

Hypothesis tests compare and asses differences between variables. In case of permeability anisotropy of particular lithofacies, we should know whether the permeability data from different depths have the same distribution or not. Hypothesis tests identify the difference between two samples, accepting or rejecting either the null hypothesis or alternative hypothesis with 95% of confidence level. Accepting the null hypothesis, we assume that sampling variability affects the difference between two samples, whereas the alternative hypothesis shows that the difference cannot be explained by sample variability (Jensen *et al.,* 2003). Confidence level is used to avoid error while accepting or rejecting the null and alternative hypotheses, because we can reject the null hypothesis when it is true.

# CHAPTER III
# GEOLOGY

## 3.1 Introduction

Heidrun field is one of several prolific hydrocarbon reservoirs within Halten terrace in the North Sea, offshore Norway. An important productive formation is the Early Jurassic Tilje Formation. The structural history of the Halten terrace includes a long history of subsidence and rifting from the Triassic to Early Eocene that defined the Norwegian-Greenland Sea Rift. The Tilje Formation comprises late-stage, pre rift basin deposits formed during the opening of the mid-Atlantic rift system accumulation which developed as a results of thermal subsidence and sedimentary compaction.

The geology, petrology, depositional environments, and reservoir characteristics of the Tilje Formation have been studied previously (Whitley, 1992, Martinius *et al.*, 1999 and 2001). Martinius *et al.* (2001) interpret depositional processes of the formation and internal facies. Their work is used here to define rock types (lithofacies) that may have distinct reservoir properties.

Isotope analysis carried out by Statoil identified three main sedimentary sources formed the Tilje Formation (Martinius *et al.,* 2001). The first and most important source was mainland eastwards of the Tröndeldag platform. The remaining sediments came from the north (Ribbab basin), which was influenced by erosion during the entire Jurassic, and from the west (Helland-Hansen-Bodø high).

The thickness and diversity of depositional facies in the Tilje Formation reflect local variations in subsidence rate and complex depositional patterns in a shallow, wave-, storm-, and tide-influenced seaway (Martinius *et al.*, 2001). Ten lithofacies associations were identified within Tilje Formation:

1. Basin floor.
2. Transgressive.
3. Prodelta heterolithic.
4. Distal delta front lobe.

5. Outer estuarine and delta front bar.
6. Channalised delta-front lobe.
7. Inshore estuarine.
8. Heterolithic tidal flat channel.
9. Tidal channel.
10. Lower delta plain.

Rock-property data are available for only seven lithofacies (1-4, 6, 7 and 9). Martinius *et al*. (1999) indicate that tidal channel and shoal facies (lithofacies 6 and 7) have the best reservoir properties. Other lithofacies composed of sandstone layers with good reservoir properties are complicated by interbedded mudstone/siltstone layers.

### 3.2 Lithofacies associations

A conceptual depositional model showing the approximate location of the facies associations (Figure 3-1) suggests that facies described below are located on lower delta plain, delta-front, and prodelta parts of a delta.

***Lithofacies Association 1 - Basin floor facies***

This lithofacies association, at the base of the Tilje Formation, is composed of intensly bioturbated muds and very fine-grained sandstone. Fine grain size reflects a low-energy depositional environment. Some layers contain up to 1-m-thick calcified deposits, and sediments are rich in muscovite and biotite.

***Lithofacies Association 2 - Transgressive facies***

Deposits formed at the transition from shallow, marginal marine sediments to relatively deepwater, open marine environments (Martinius *et al.,* 2001). Deposits are poorly sorted and include locally abundant angular calcite grains. The deposits are a mix of mudstone, sandstone, and shell debris.

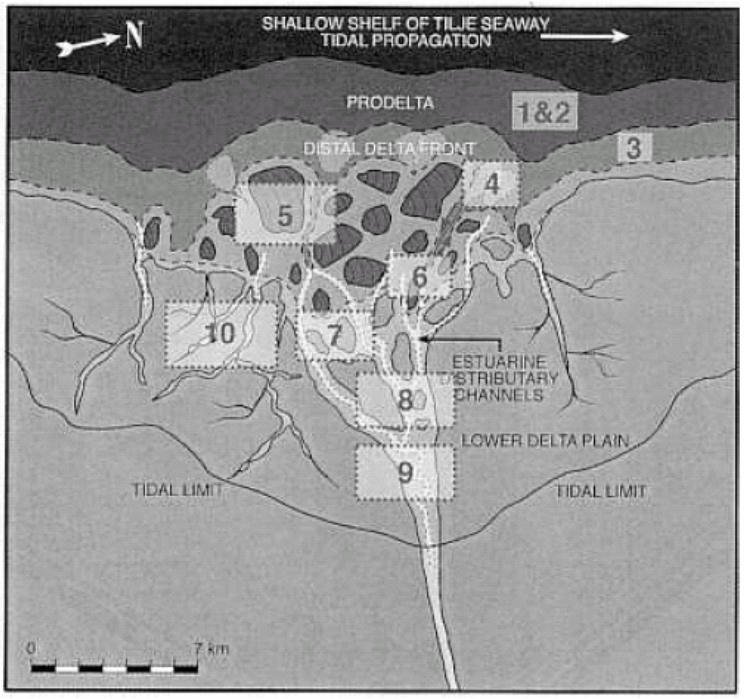


**Figure 3-1.** Approximate location of the lithofacies association within the conceptual depositional model (Martinius *et al.*, 2001)

***Lithofacies Association 3 - Prodelta heterolithic facies***

Pairs of layers consisting of one sandstone or siltstone and one mudstone suggest that these deposits were formed in a tidal regime. Lithofacies 3 are interpreted to be quiet-water; mud-rich, delta-front facies characterized by slow deposition from suspension and occasional rapid deposition of coarser sediment by traction currents during river floods (Martinius *et al.,* 2001). Thin mudstone, siltstone, and very fine-grained sandstone layers have almost equal thickness.

Small-scale cracks filled with sand from overlying layers are common. Although the origin of cracks is debatable, they are interpreted to be subaqueous.

***Lithofacies Association 4 – Distal delta front lobe facies***

Lithofacies Association 4 was interpreted to be deposits formed in a low-relief deltafront, on distributary channel-mouth bars, and associated with expanding flows (Martinius *et al.,* 2001). Proximal deposits are sandier, and more distal deposits contain

abundant, relatively thick, more regularly spaced mudstone layers. Sandstones are mica-rich, and contain double mud drapes and siderite layers.

***Lithofacies Association 6 – Channelised delta-front lobe facies***

Lithofacies 6 consists mostly of medium-grained, small-scale, cross-stratified sandstone with double mud drapes. Bioturbation, which causes feather-like mud layers, is common in some locations. Crossstratification was formed by migrating, small-scale dunes and current ripples within channels located at the end of delta distributaries.

***Lithofacies Association 7 – Inshore estuarine facies***

Lithofacies 7 consists of well-sorted, fine-grained sandstones with flaser-bedded sandstone layers. This lithofacies is laterally extensive across a 3-km-wide belt, suggesting deposition over a relatively large, shallow estuarine region.

The depositional environment has been interpreted as indicative of both wave- and tidal-current processes because flaser bedding reflects deposition in the deeper, subtidal parts of ebb- and flood-dominated channels and estuarys.

***Lithofacies Association 9 – Tidal channel facies***

Lithofacies Association 9 is thin gravel layers above the base of a channel. Restricted bioturbation suggests low salinity.

This lithofacies association is composed of three lithofacies, which are subdivided on the basis of the sorting and grain size. Deposits of lithofacies association 9 are characterized by two superimposed upward-fining successions: one small-scale variant comprising occurrence of lithofacies 9.1, which is included in this study, and a large-scale variant.

### 3.3 Petrology and diagenesis

Petrology and diagenesis of the Tilje Formation reflect two factors that significantly influence the issue of porosity and permeability distribution. Muscovite clasts and carbonaceous fragments are concentrated in the finer fractions of some lithofacies (Whitley, 1992). Abundance of siderite cement occurs in the upper few meters of the formation, reducing porosity. The other important factor affecting the permeability is the type of clay. X-ray diffraction revealed that kaolinite is the dominant clay (Whitley, 1992); although some traces of illite and chlorite are defined, they do not influence production.

# CHAPTER IV
# AVAILABLE DATA

## 4.1 Introduction

Available data are divided into categories and briefly described below. Each set of data played an important role in the analysis and interpretation of the present study. The majority of the petrophysical data consists of core information from the Well D, Tilje Formation, Heidrun Field.

## 4.2 Sedimentological description

Depositional environments of the Tilje Formation were controlled by the structural setting, providence of the sediments. There, in turn, changes in grain size and mineralogical composition influenced the permeability and permeability anisotropy of lithofacies. Lithofacies are described in Chapter II. Well-logs and cores were subdivided into lithofacies by workers at Statoil Research Center.

## 4.3 Log data

Log data included density, neutron, gamma-ray, and sonic, interpreted lithofacies, permeability, log of permeability, fraction of porosity and volume of shale. The well-log information was helpful in depth shifting, which was used to evaluate the properties of the reservoir rocks and interpret the heterogeneity of a particular lithofacies.

## 4.4 Core plug data

Of 302 core plugs, 244 were horizontal and 62 were vertical (Table 4-1). The number of samples for every facies varies depending on the thickness and abundance of the lithofacies. Horizontal plugs were sampled every 0.3 m with some gaps. Sampling intervals for vertical plugs vary. Core plug permeability data are the essential part of all

analysis conducted, and models were constructed to evaluate the permeability anisotropy of the Tilje Formation.

**Table 4-1**. Total number of the horizontal and vertical permeability data

| *Association* | Lithofacies | $k_h$ | $k_v$ |
|---|---|---|---|
| 1 | Basin floor facies | 41 | 11 |
| 2 | Transgressive facies | 4 | 1 |
| 3 | Prodelta heterolithic facies | 20 | 4 |
| 4 | Distal delta front lobe facies | 45 | 12 |
| 6 | Channalised delta-front lobe | 12 | 0 |
| 7 | Inshore estuarine | 8 | 3 |
| 9 | Tidal channel facies | 114 | 31 |
| | **Total** | **244** | **62** |

## 4.5 Minipermeameter data

Minipermeameter data were collected to study the detailed small-scale petrophysical properties of bedding within different lithofacies (Martinius *et al.,* 1999). Five intervals of minipermeameter data are available. Minipermeameter grids were measured using a 2-mm x 2-mm-inner-diameter probe tip (Martinius *et al.*, 1999). Table 4-2 presents statistical data summarizing these measurements. Although a large number of measurements were collected from minipermeametry, only plots (Figure 4-1) of the probability distribution function (PDF) of minipermeameter measurements were available. Four of seven lithofacies were sampled by the minipermeameter. A comparison of probe and plug data provides information on small-scale rock heterogeneity.

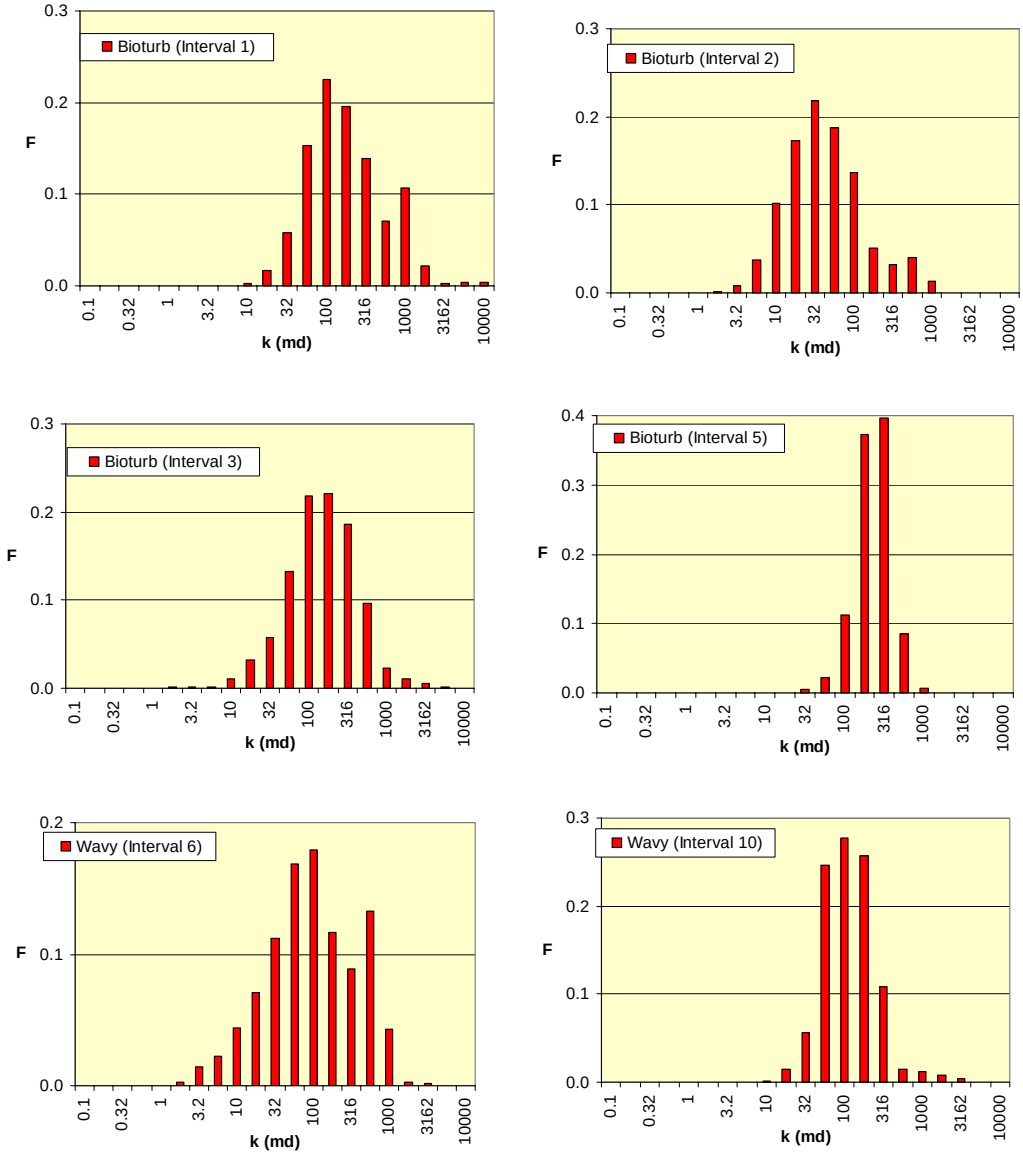


**Figure 4-1.** Histograms of the minipermeameter probe-permeability data (taken from Statiol report)

**Table 4-2.** Statistical data for minipermeameter data

| | | N | Cv | SE | Mean |
|---|---|---|---|---|---|
| **Tidal flat** | **Interval 6** | 3096 | 1.32 | 3.62 | 152.5 |
| **Tidal channel** | **Interval 10** | 1069 | 1.54 | 5.85 | 124.4 |
| **Delta lobe** | **Interval 1** | 2296 | 2.24 | 12.98 | 277.1 |
| | **Interval 2** | 3110 | 1.67 | 1.99 | 66.2 |
| | **Interval 3** | 2600 | 1.48 | 5.27 | 181.5 |
| | **Interval 5** | 2852 | 0.51 | 1.81 | 190.2 |

### 4.6 Additional data

To clearly see and understand how the sedimentological settings of the lithofacies affect the core plug and minipermeameter data, core photos were obtained from Martinius *et al.*, (2001) and from the official Website of Norwegian Petroleum Directorate.

# CHAPTER V
# PERMEABILITY ANALYSIS

## 5.1 Introduction

This chapter discusses data analysis conducted to understand the nature of the permeability variation, to assess the permeability anisotropy, and to define a permeability anisotropy model of the Tilje Formation.

## 5.2 Depth shift and matching

Lithology of the rock affects the vertical and horizontal permeability. Precise correlation between welllogs and core plug permeability measurements is necessary to obtain information on how the reservoir rock properties of influence permeability. Incorrect depth matching can lead to erroneous results during further analysis and to misinterpretation of the permeability anisotropy of the lithofacies. The main principle is to match the permeability data with welllogs [gamma ray (GR) and bulk density (RHOB)] that indicate the lithology of the reservoir. The core plug permeability data were listed with measured depths whereas the log data were in true vertical depth.

Sedimentological descriptions were available for the core plug and log data, which was helpful during depth matching. I divided the matching procedure into two steps. In the first, I used sedimentological descriptions, and in the second, I compared the core data with log data point by point.

Well-log data were sampled each 0.15 m, whereas core plug sampling intervals varied from 0.3 m to about 0.9 m. The first step of depth matching done on the basis of the sedimentological description of the core and well-logs is shown in Figure 5-1. The depth mismatch is apparent because of the influence of the lithology of the rock on the RHOB reading. The first step of the depth match used a conventional log analysis program. The program, however, was not able to shift on small scales, so I used Excel to match the RHOB and GR data with the core permeability data (Figure 5-2).

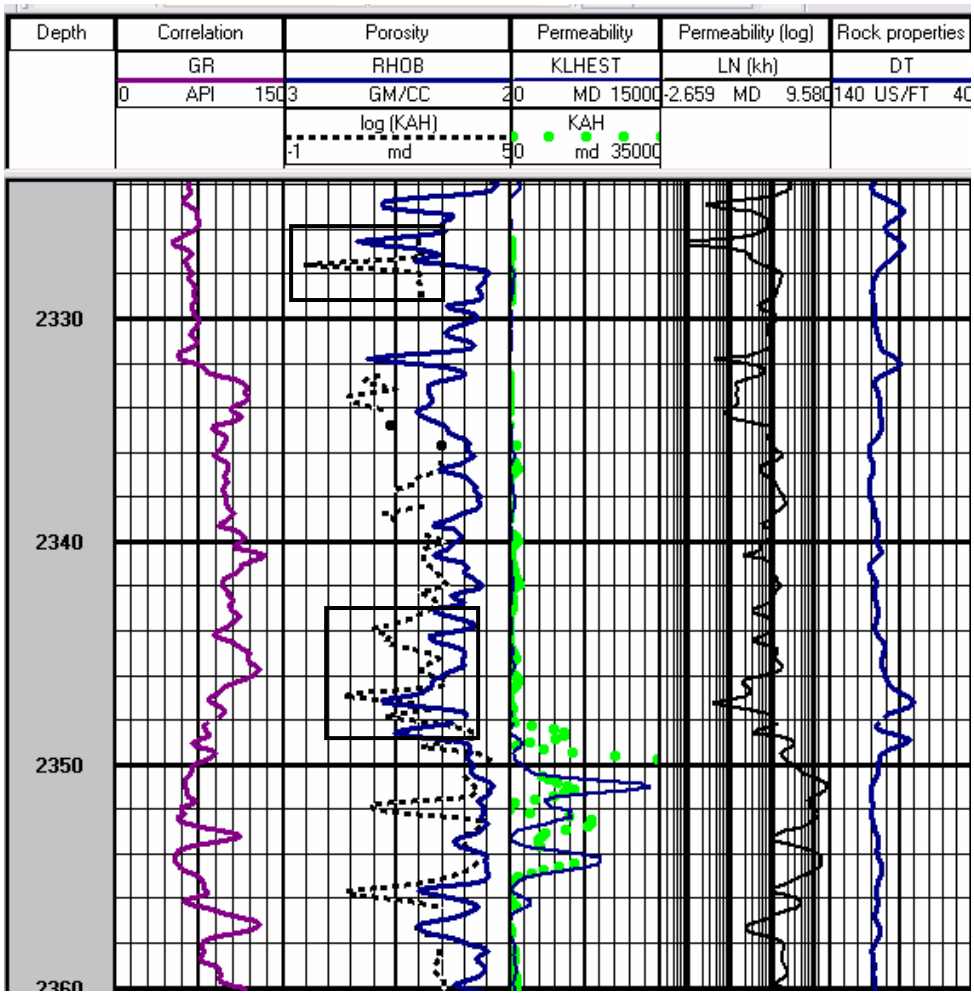


**Figure 5-1.** Rectangles show apparent mismatch between RHOB and core permeability after first step of depth shift

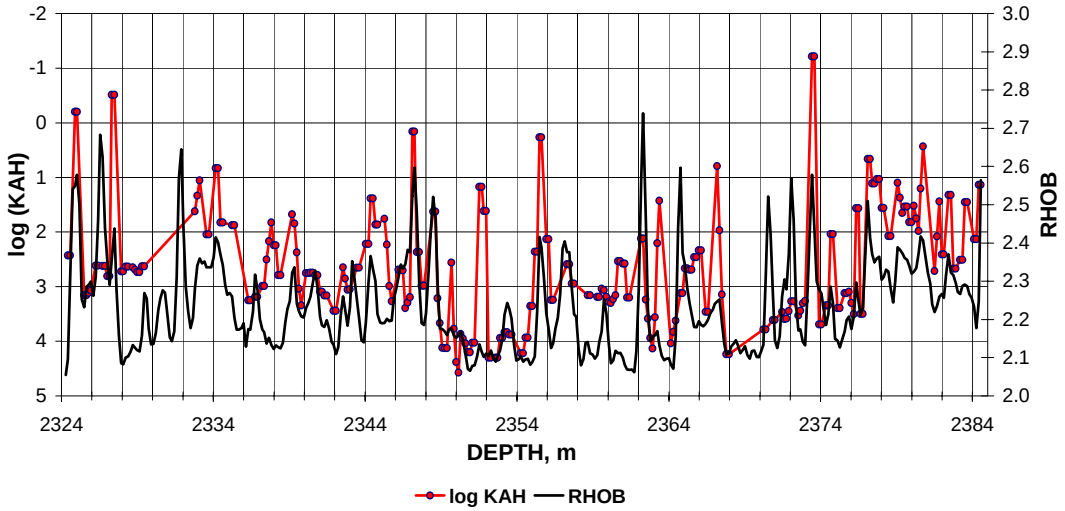


**Figure 5-2.** Fairly good correlation achieved between core permeability and RHOB after second step of correlation procedure

***Discussion on depth shift and matching***

The appropriate interpretation of further analysis of the reservoir heterogeneity could be conducted only after the correct depth matching. Reservoir heterogeneity has been recognized as an important factor in determining reservoir properties, such as permeability, that can be evaluated by comparison of well-log data and permeability data. The match achieved between core and log data is fairly good. To improve the correlation, additional information, such as core pictures and the real core observation, would be helpful. Core pictures obtained from the published literature and Norwegian Petroleum Directorate (NPD) Website are from other wells through the Tilje Formation.

## 5.3 Permeability characteristics of lithofacies

General characteristics of the permeability distribution in subsets from different depths within the core are given in Figure 5-3. Although subsets contain different numbers of core plug measurements, the distributions of permeability measurements within subsets are similar. I conducted a comparative analysis was conducted to merge them into a single set of permeability measurements for each lithofacies.

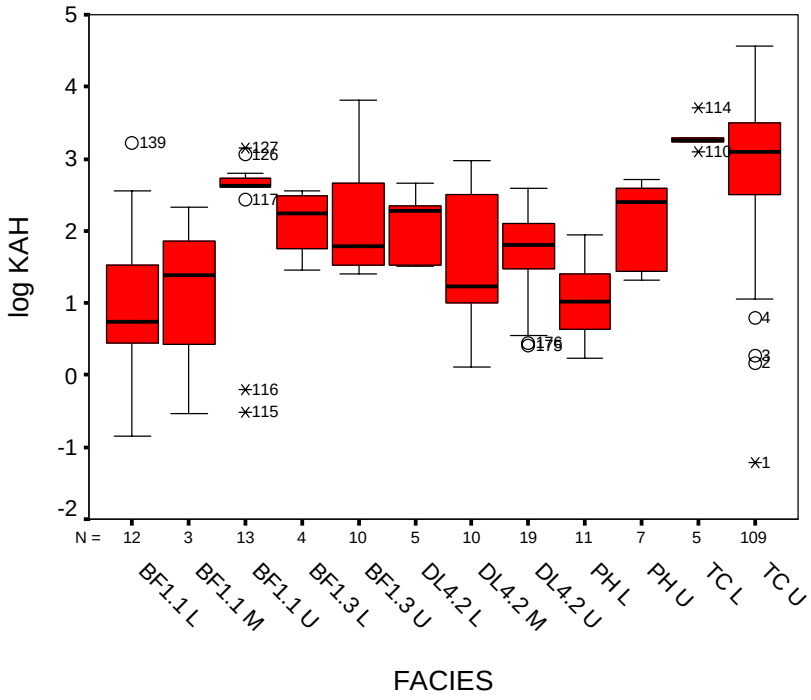


**Figure 5-3.** Subsets of the lithofacies (BF 1.1 and 1.3 – Basin floor lithofacies 1.1 and 1.3, DL 4.2 – Delta lobe lithofacies 4.2, PH – Prodelta heterolithoc, TC – Tidal channels, U – from upper part of the core, L – from lower part of the core, M – from middle part of core, N – number of core plugs in subset)

## 5.4 Comparative analyses of lithofacies permeabilities

The purpose of hypothesis testing is covered briefly in Chapter II of the thesis. I used two types of hypothesis tests, the *t*-test and the Kolmogorov-Smirnov test. The *t*-test is a parametric test and Kolmogorov-Smirnov test is a nonparametric test.

For the *t*-test, the null and alternative hypotheses are used to compare the mean ($\mu$) values of two variables. The null hypothesis assumes that the two distributions have a similar mean, whereas the alternative hypothesis is that the means of the distributions are different. Two situations can be considered for the alternative hypothesis where $\mu_1 > \mu_2$ and $\mu_2 > \mu_1$. I used the "two-tailed" *t* test which allows for either $\mu_1 > \mu_2$ or $\mu_2 > \mu_1$.

The *t* test compares the absolute value of *t* (**Eq.1**) with *df* degree of freedom (**Eq. 2**), with the value obtained from statistical tables (Neave, 1978, Neave and Worthington , 1988). The value from the table has a distribution $t(\alpha/2, df)$, where $\alpha$ is the confidence

level (here, $\alpha$ = 0.05). When the absolute values of $t$ are greater than the value from the table, we reject the null hypothesis and accept the alternative hypothesis.

$$t = \frac{\overline{X_1} - \overline{X_2}}{\sqrt{\hat{s}\left(\frac{1}{I_1} + \frac{1}{I_2}\right)}} \quad \text{..... (1)}$$

$$df = \left(I_1 + I_2 - 2\right) \quad \text{..... (2)}$$

where

$I_i$ – size of the $i^{th}$ data set.

$\overline{X}_i$ - mean value of the sample.

$\hat{s}$ - unbiased estimate of $\sigma^2$.

$\sigma^2$ – variance of the set.

$df$ – degrees of freedom.

The Kolmogorov-Smirnov hypothesis test is used to compare the cumulative distribution functions (CDFs) of two variables. For this particular test, we can accept or reject the null hypothesis by comparing the maximum distance (*D,* Eq. 3) between the CDFs and tabulated critical values (Jensen *et al.,* 2003). We can reject the null hypothesis when the critical value exceeds the maximum distance (in this case at the 5% level).

To approximate the critical value ($Z_c$) at the 5% level of the confidence and calculate the maximum distance ($D$), Eq. 4 (Jensen *et al.,* 2003) is used:

$$D = I_1 I_2 d_{\max} \quad \text{..... (3)}$$

$$Z_c = 1.36\left(I_1 I_2\right)^{1/2} * \left(I_1 + I_2\right)^{1/2} \quad \text{..... (4)}$$

where

$I_i$ – size of the $i^{th}$ data set.

$d_{max}$ – maximum distance between CDFs.

The disadvantage of the *t* test is that it only compares the means of the variables. It is well-known that variables with similar means can have different distributions. The Kolmogorov-Smirnov test has the ability to comprehensively evaluate the difference of the CDFs of two variables. The disadvantage of the Kolmogorov-Smirnov test is that it is designed to detect any kind of differences in distribution, regardless of changes in location or dispersion (Neave and Worthington, 1998).

### 5.5 Horizontal core plug permeability

The location of permeability data from each lithofacies is shown in Figure 5-4. A comparison of the permeability data from different positions in the core for each lithofacies was needed to determine if lithofacies permeability values vary with depth.

Mean permeability values measured from similar lithofacies at various depths in the core were compared. The results (Table 5-1) show that all sets of the same lithofacies have similar means. Thus, I combined the data from different depths to conduct further analysis.

**Table 5-1.** All analyzed lithofacies have the same mean

| Lithofacies | Sections | Table | Absolute "t" |
|---|---|---|---|
| **Basin floor 1.1** | Upper vs. Middle section | 2.145 | 0.0897 |
| | Middle vs. Lower section | 2.160 | 0.7233 |
| | Upper vs. Lower section | 2.069 | 0.0738 |
| **Basin floor 1.3** | Upper vs. Lower section | 2.179 | 0.5606 |
| **Prodelta** | Upper vs. Lower section | 2.120 | 0.0045 |
| **Delta lobe 4.2** | Upper vs. Middle section | 2.052 | 0.2531 |
| | Middle vs. Lower section | 2.160 | 0.9656 |
| | Upper vs. Lower section | 2.074 | 0.1069 |
| **Tidal channel** | Upper vs. Lower section | 1.156 | 0.6816 |

To strengthen my conclusion that permeability measurements from the same lithofacies at various depths were similar, I conducted the Kolmogorov-Smirnov

hypothesis test (Table 5-2). Comparing the critical values and maximum distance of the core permeability data sets from different sections of the core for particular lithofacies, I concluded that the permeability data for each lithofacies at different depths has the same distribution (Table 5-2). These test results allowed me to combine the data and conduct further analysis.

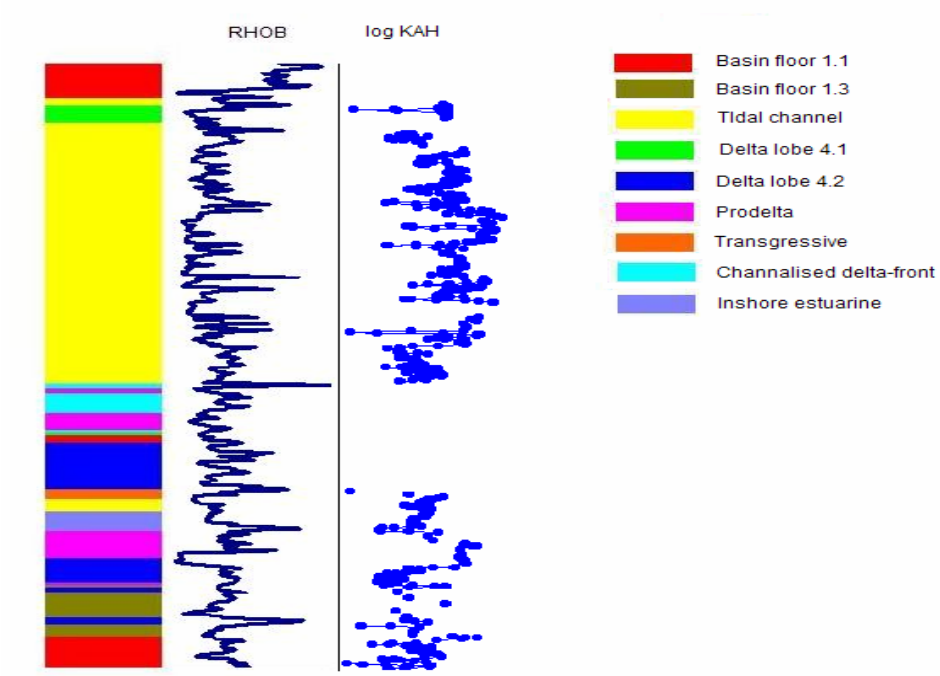


**Figure 5-4.** Location of lithofacies of the core (RHOB and log KAH are not in appropriate scale)

***Comparing the lithofacies from the lithofacies associations***

I also conducted the Kolmogorov-Smirnov test to evaluate the similarity of permeabilities of lithofacies (Basin Floor 1.1 and 1.3 and Delta Lobe 4.1 and 4.2) from the same lithofacies association. The results of the analysis (Table 5-3) reveal that core permeability sets have the same distribution. The similarity of Basin floors 1.1 and 1.3 is questionable, because Basin Floor 1.1 is intensively bioturbated while Basin Floor 1.3

has preserved layering (Appendix A). Sampling could be an issue of the similarity if the core plugs from Basin Floor 1.1 were sampled from sandier parts of the core, which is impossible to prove because the core is not available for observation.

**Table 5-2.** Analyzed lithofacies come from the same distribution

| Lithofacies | Sections | Critical values | Maximum distance |
|---|---|---|---|
| **Basin floor 1.1** | Upper - Middle section | 33.97 | 22.00 |
| | Middle - Lower section | 31.60 | 29.88 |
| | Upper - Lower section | 84.93 | 81.50 |
| **Basin floor 1.3** | Upper - Lower section | 32.18 | 25.00 |
| **Prodelta** | Upper - Lower section | 50.63 | 38.50 |
| **Delta lobe 4.2** | Upper - Middle section | 100.95 | 65.00 |
| | Middle - Lower section | 37.25 | 25.00 |
| | Upper - Lower section | 64.94 | 30.00 |
| **Tidal channel** | Upper - Lower section | 338.99 | 161.00 |

Based on core plug data, I constructed histograms of horizontal permeabilties for each lithofacies (Figure 5-5) except the Transgressive lithofacies, which have very few data points (Table 4-1).

**Table 5-3.** Both lithofacies have the same distribution

| Lithofacies | Critical values | Maximum distance |
|---|---|---|
| **Basin floor** | 190.94 | 164.00 |
| **Delta lobe** | 145.36 | 102.00 |

The Tidal channel and Inshore estuarine lithofacies show the highest permeability values, supporting the conclusions of Martinius *et al.* (1999). Basin floor, Prodelta heterolithic, and Delta lobe lithofacies have wide ranges of permeability (Figure 5.5a-c).

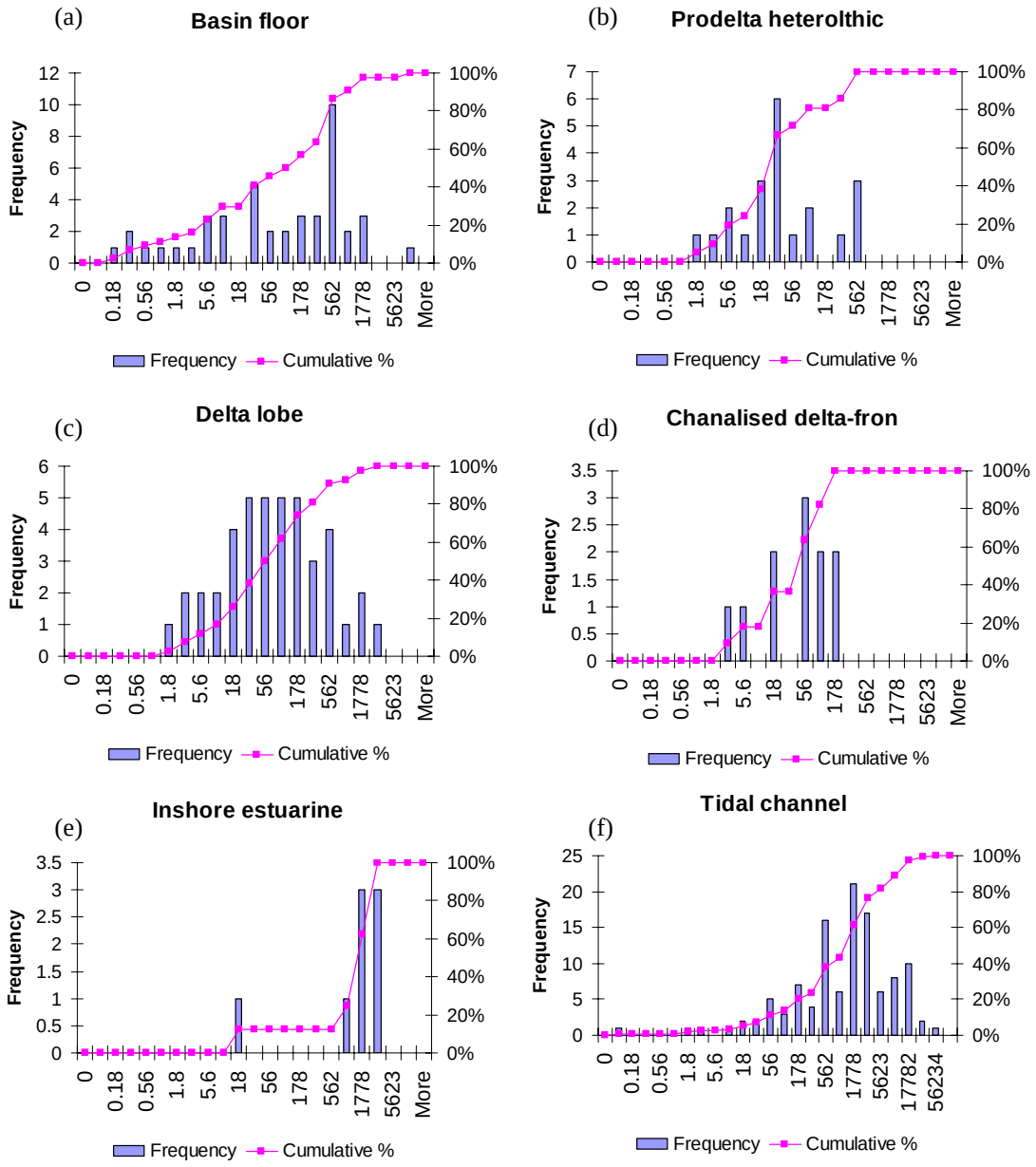


**Figure 5-5**. Histograms of the core plug horizontal permeability for six lithofacies

The permeability distribution for the Basin floor lithofacies probably reflects intensive bioturbation. Prodelta heterolithic lithofacies were deposited in a setting where thin mud and fine-grained sandstone layers were interbedded (Martinius *et al.,* 2001); the bimodality of the histogram reflects these low- and high-permeability layers.

Using the sets of core plug permeability data, I calculated several statistical variables (Table 5-4). The Tidal channel and Inshore estuarine lithofacies show the highest mean and median values. The Inshore estuarine lithofacies also has high mean and median values. Minimum permeabilities are very small values in all lithofacies. The significant difference between statistical values might reflect the lithological origin or the effect of the depositional setting of the lithofacies. Some lithofacies, such as Tidal channel lithofacies, they constitute less than 10% of the data set.

**Table 5-4.** Statistics of the horizontal core plug permeability (in md)

| **No.** | 1 | 3 | 4 | 6 | 7 | 9 |
|---|---|---|---|---|---|---|
| **Lithofacies** | **Basin Floor** | **Prodelta heterolithic** | **Delta lobe** | **Channalised delta-front** | **Inshore estuarine** | **Tidal channel** |
| **N** | 44 | 21 | 42 | 11 | 8 | 114 |
| **Min** | 0.14 | 1.75 | 1.28 | 2.68 | 14.4 | 0.06 |
| **Max** | 6430 | 516 | 2200 | 135 | 2220 | 37100 |
| **Mean** | 404.95 | 92.92 | 240.70 | 50.69 | 1439.68 | 3385.59 |
| **Median** | 84.35 | 23.70 | 58.25 | 34.10 | 1530.00 | 1305.00 |
| **SD** | 1005.52 | 156.30 | 486.06 | 46.68 | 739.42 | 5580.10 |
| **Cv** | 2.5 | 1.7 | 2.0 | 0.9 | 0.5 | 1.6 |

Martinius *et al.* (2001) mentioned calcified layers within tidal channels (discussed in the following section). The histogram of the horizontal permeability of the Tidal channel lithofacies (Fig 5-5f) suggests that the permeability values are probably associated with calcite layers. As the lithofacies consists of channel bodies, a plot of horizontal permeability versus GR (Figure 5-6) helped to allocate the points within channels at the top of the coarsening-upward sequences (the two arrows on the plot show the upward-coarsening sequences; others are too small to indicate on the plot). A plot of

the bulk density of the smallest permeability values versus depth (Figure 5-7) shows that the three of the five points have relatively close values of bulk density, which suggests a similarity of the rocks at different depths. The intensity of the calcite cement increases with depth (Figure 5-8), which is suggested by the deepest lower-permeability point with the highest RHOB value.

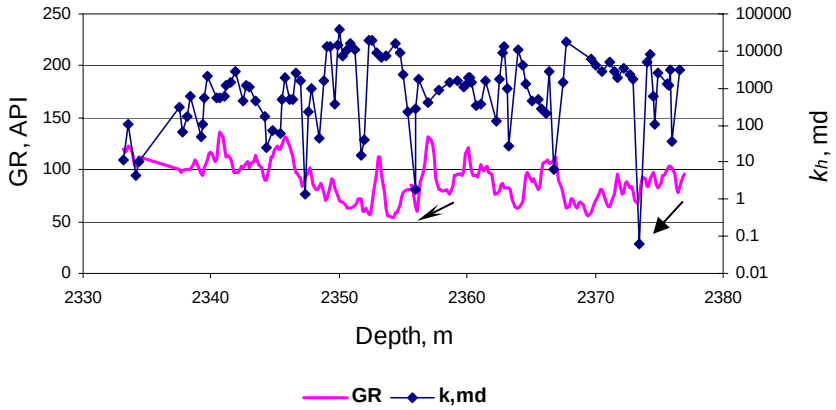


**Figure 5-6.** Small permeability values located at top of channel bodies

Only one of the five points, having the lowest RHOB value, appears to be porous sandstone. Reduction of the horizontal permeability at this point is the effect of the lithology. The low permeability value in the sandstone interval suggests that not only the calcite layers have a dramatic impact on the horizontal permeability.

Variation of lithofacies lithology can be examined by analyzing the well-log data (Figure 5-9). The Tidal channel lithofacies displays a wide range of GR values, suggesting heterogeneity that affected the permeability of some horizontal core plugs. Inshore estuarine and Channlised delta lithofacies display a narrow range of GR values (Figure 5-9) and both lithofacies have almost equal values of the mean and median. The range of permeability values for the Basin floor lithofacies can be correlated along with dissimilarity of the horizontal permeabilities.

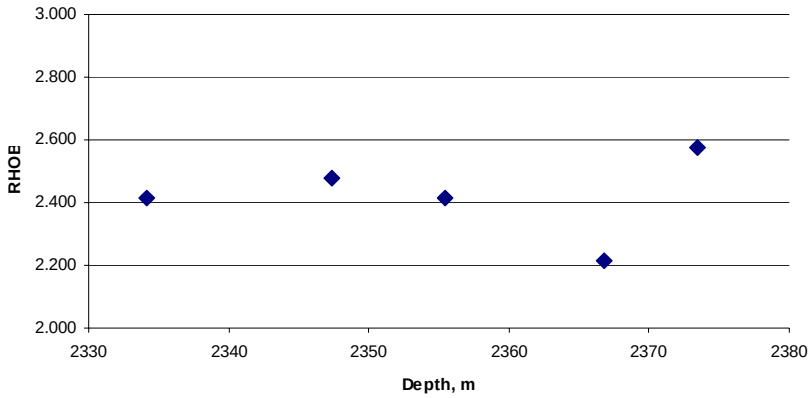


**Figure 5-7.** Most small permeability values shows the relatively similar bulk density

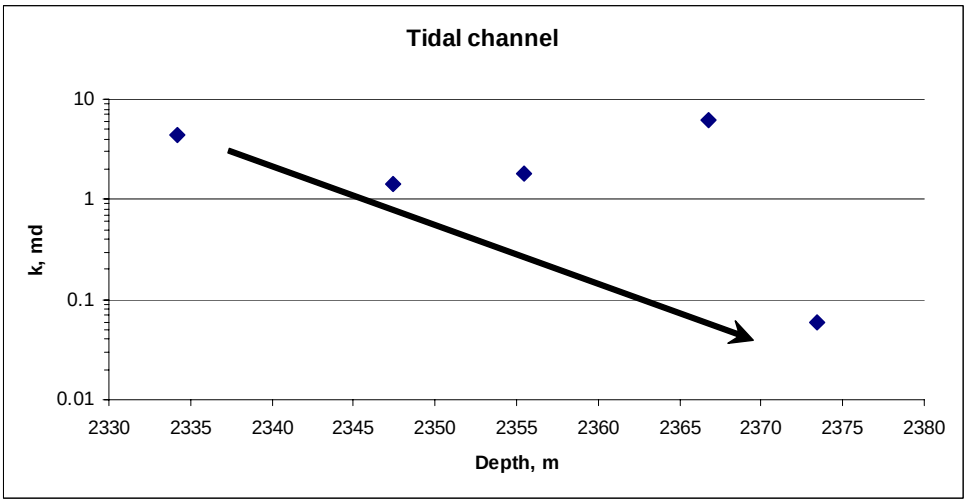


**Figure 5-8.** The intensity of carbonate cement increases with depth

***Conclusions***

Lithofacies from particular lithofacies associations have similar permeability distributions. A comparative analysis helped justify the combination of information into one set of data for each lithofacies to proceed to the further evaluation.

Considering the facts of reduced permeability of the Tidal channel lithofacies and high permeability of the Inshore estuarine and the Channalised delta-front, I concluded

that depositional settings and lithology of the lithofacies controls the permeability distribution.

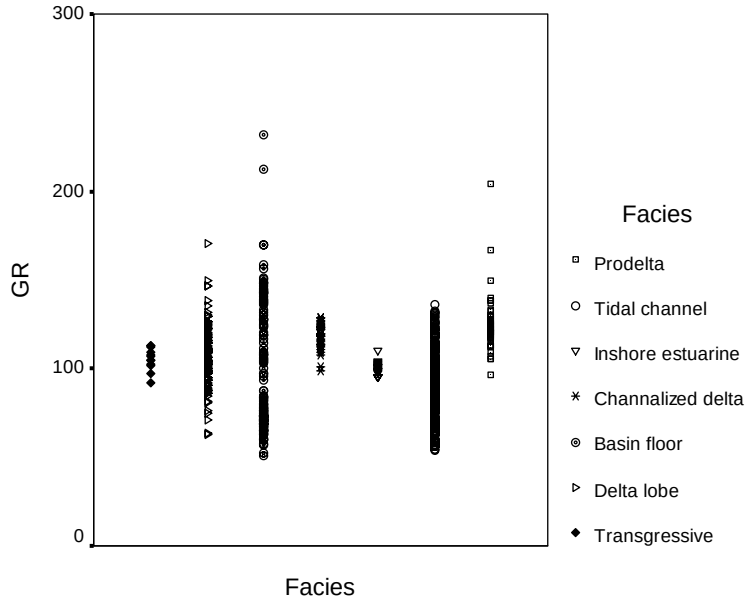


**Figure 5-9.** Lithology of the lithofacies captured by log data

### 5.6 Minipermeameter (probe) permeability

Minipermeameter data were collected from the core at six intervals and the locations of the intervals were indicated on the core description. The minipermeametry was applied to study small-scale lamination and its effect on the permeability (Martinius *et al.,* 1999). Also, probe data were gathered from different intervals of laminated sediments or having variable bioturbation.

Four sampled intervals from the Distal delta front lobe lithofacies (Intervals 1-3 and 5), one from the Prodelta heterolithic lithofacies (Interval 6), and one from the Tidal channel lithofacies (Interval 10) were examined. A comparison of the minipermeameter and core plug data used statistical information and obtained from the Statoil report (Table 5-5).

The four intervals sampled from the Delta lobe lithofacies had different arithmetic average permeabilities. Martinius *et al.* (2001) state that thin irregularly

spaced mudstone layers affect the minipermeameter measurements. There are several other causes which may have also affected the measurements; including unclean core and volume of samples (Corbett and Jensen, 1992).

**Table 5-5.** Probe permeability statistics (in md)

| | Tidal flat | Tidal channel | Delta lobe | | | |
|---|---|---|---|---|---|---|
| **Interval no.** | **6** | **10** | **1** | **2** | **3** | **5** |
| **N** | 3096 | 1069 | 2296 | 3110 | 2600 | 2852 |
| **Cv** | 1.32 | 1.54 | 2.24 | 1.67 | 1.48 | 0.51 |
| **SE** | 3.62 | 5.85 | 12.98 | 1.99 | 5.27 | 1.81 |
| **A. Mean** | 152.5 | 124.4 | 277.1 | 66.2 | 181.5 | 190.2 |

Some logs (particularly GR and RHOB) are able to capture the heterogeneity of the reservoir rock. Therefore, I used the available well-log information to evaluate how the heterogeneity is reflected in the minipermeameter measurements. I have compared the arithmetic mean probe permeabilities with welllog (GR, RHOB) readings at the same depth (Figure 5-10).

Figure 5-10 and Table 5-6 show the correlation between the GR values and arithmetic means of the minipermeameter measurements. The lowest value of GR correlates with the highest values of arithmetic mean probe permeability and vice versa. One explanation for this is that the mud content is affecting both the GR and probe measurements.

Generally, with the increase of RHOB value, one expects a decrease of permeability. This is not the case in Figure 5-10; the RHOB values are inversely related to permeability. The increase of the RHOB values leads to increase of the arithmetic mean of the interval. There could be several causes for this reverse relationship, including: depth mismatch and incorrect reading of the logging tool at the interval. Without further information, such as photos, we cannot identify the cause.

***Conclusions***

Observed that the lithology and depositional settings influenced minipermeameter measurements. The correlation between probe permeability values and GR log values suggests that increased GR values are associated with lower permeability. The factors affecting the relationship between the RHOB and probe-permeability are unknown.

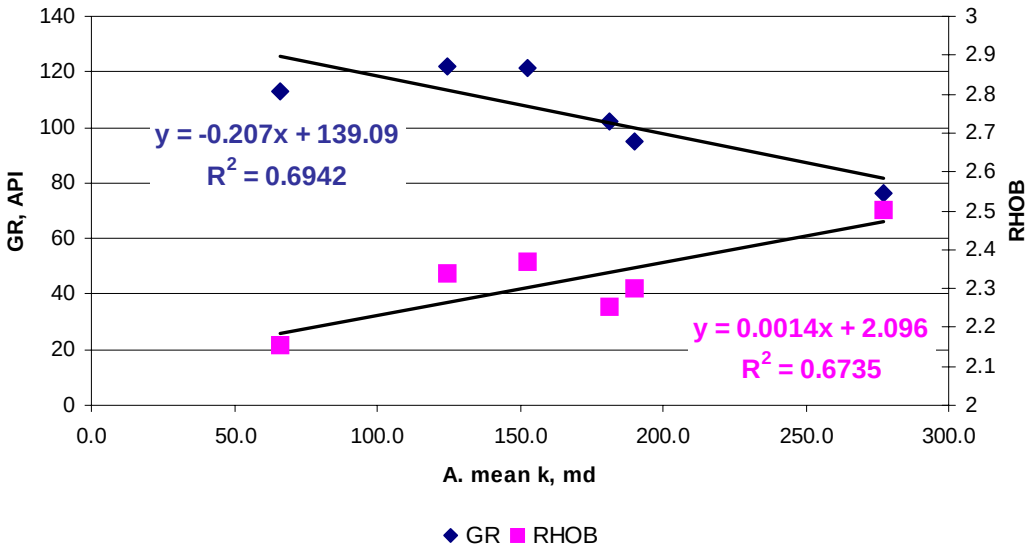


**Figure 5-10**. Arithmetic mean of probe data shows a good correlation with GR

**Table 5-6.** Comparison table

| Lithofacies | Intervals | Mean (md) | GR |
|---|---|---|---|
| Tidal flat | Interval 6 | 152.5 | 121.111 |
| Tidal channel | Interval 10 | 124.4 | 122.04 |
| Delta lobe | Interval 1 | 277.1 | 76.348 |
| | Interval 2 | 66.2 | 112.83 |
| | Interval 3 | 181.5 | 102.18 |
| | Interval 5 | 190.2 | 94.69 |

### 5.7 Comparison of horizontal plug and probe permeabilities

To compare probe and plug data, I conducted a Kolmogorov-Smirnov hypothesis test (Table 5-7). The test revealed that these different measurement methods resulted in different permeability distributions. Corbett and Jensen (1992) indentified several reasons for core plug and probe differences. The following part of the chapter presents several analyses that were conducted to interpret and understand the nature of these differences in terms of geological, statistical, and well-log information. The sedimentological setting of the lithofacies was useful in interpreting these results.

**Table 5-7**. Results of Kolmogorov-Smirnov hypothesis test

| Lithofacies | Plug vs. Probe | Critical values | Maximum distance |
|---|---|---|---|
| Delta lobe | Core plug vs Interval 1 | 18341.81 | 23796.00 |
| | Core plug vs Interval 2 | 24797.04 | 26082.00 |
| | Core plug vs Interval 3 | 20752.62 | 25686.00 |
| | Core plug vs Interval 5 | 22751.04 | 48684.00 |
| Prodelta | Core plug vs Interval 6 | 24686.02 | 31316.37 |
| Tidal channel | Core plug vs Interval 10 | 8611.03 | 30051.53 |

Heterogeneity may affect the sampled permeability values. Comparison of the coefficients of variation ($C_v$s) was used to estimate the heterogeneity measured from the probe and core plug data (Table 5-8)**.** Overall, Interval 1 of the Delta lobe lithofacies has the highest heterogeneity which is reflected in the small number of highest-permeability values observed on the histograms (Figure 4-1). The $C_v$ values of the probe and core plug data do not differ significantly, so they appear to represent similarly heterogeneous reservoir rock, in spite of the difference of the sampling volume.

Table 5-9 shows differences between the average core plug and probe permeabilities. Four intervals (Intervals 1-3 and 5) were sampled from the Delta lobe lithofacies (Table 5-9). Three of the four sampled intervals have lower mean probe than core plug permeability. The lowest mean probe-permeability values from Interval 2

correlates with highest values of GR, suggesting that these measurements were taken from muddier parts of the lithofacies.

**Table 5-8.** Heterogeneity measurements of probe and core plug data

| | | Cv | | |
|---|---|---|---|---|
| **No.** | **Lithofacies** | **Core plug** | **Probe** | **Intervals** |
| 1 | Basin floor | 2.5 | No sample | |
| 3 | Prodelta heterolithic | 1.7 | 1.32 | Interval 6 |
| 4 | Delta lobe | 2.0 | 2.24 | Interval 1 |
| | | | 1.67 | Interval 2 |
| | | | 1.48 | Interval 3 |
| | | | 0.51 | Interval 5 |
| 6 | Channalised delta-front | 0.9 | No sample | |
| 7 | Inshore estuarine | 0.5 | No sample | |
| 9 | Tidal channel | 1.6 | 1.54 | Interval 10 |

**Table 5-9.** Comparison table of means and GR

| | | | Mean | | GR | |
|---|---|---|---|---|---|---|
| **No.** | **Intervals** | **Lithofacies** | **Core plug** | **Probe** | **Core plug** | **Probe** |
| 3 | Interval 6 | Prodelta heterolithic | 92.9 | 152.5 | 117-204 | 121.1 |
| 4 | Interval 1 | Delta lobe | 240.7 | 277.1 | 63-171 | 76.348 |
| | Interval 2 | | | 66.2 | | 112.83 |
| | Interval 3 | | | 181.5 | | 102.18 |
| | Interval 5 | | | 190.2 | | 94.69 |
| 9 | Interval 10 | Tidal channel | 3385.6 | 124.4 | 57-136 | 122.0 |

Only one interval (Interval 6) was sampled at the Prodelta heterolithic lithofacies. In contrast to the Delta lobe facies, the minipermeameter data reveal higher mean permeability values than the core plug data. The description given by Martinius *et al.* (2001) mentions that this lithofacies has unique sedimentological structure and consist of approximately equal thicknesses of mudstone and siltstone or very fine-grained sandstone layers. Having the higher volume, the core plug can consist of several high-

and low-permeability layers; since the Prodelta heterolithic lithofacies exposes a layered system (Appendix A) that, in its turn, reduces horizontal permeability, I concluded that the volume of the sample played a significant role.

A similar situation is observed comparing probe and core plug averages of the Tidal channel lithofacies. Minipermeameter measurements revealed much lower values (an order of magnitude) than core plug permeability. Only one interval (Interval 10) was sampled from this lithofacies. Apparently, this facies consists of clean sands and has permeabilities an excess of 10000 md. Martinius *et al.* (2001) state that bioturbation is sparse. This interval may have been sampled close to cross-stratified layers or bioturbation, even though its GR is high. Thus, core plugs were taken from sandier parts of the core.

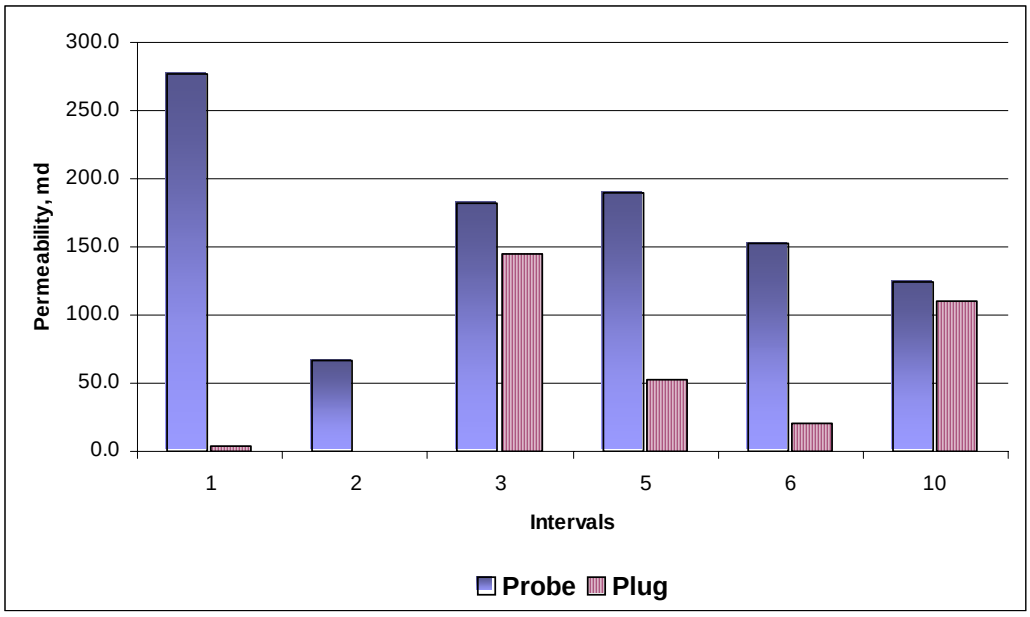


**Figure 5-11.** Difference between plug and probe data is obvious

To illustrate the ideas mentioned above, I compared the plug data and probe data at the same location. Figure 5-11 gives visual evidence that in most cases the core plug

permeability is significantly lower than the probe measurements and appears to show that the permeability is affected by the scale of measurement. Minipermeameter measurement sample small-scale volumes and thus cannot measure effects of large-scale heterogeneity. Core plug measurements sample a number of high- and low-permeable layers, reducing overall the permeability of the plug.

***Conclusions***

Statistically measured heterogeneities of the probe and core plug permeabilities are fairly close. Different scales of sample measurements are capturing the heterogeneity of the reservoir rock. However, the rest of the analysis revealed important dissimilarities. Several factors could affect the minipermeameter measurements, such as lithology of the sampled interval, size of the tip used, condition of the core, and volume of the sample (Corbett and Jensen, 1992). Another reason for dissimilarities might be the limited data.

**5.8 Vertical core plug permeability**

Sixty-two vertical core plugs were collected from the core (Table 4-1). A few samples were collected from Transgressive, Prodelta heterolithic, and Inshore estuarine lithofacies and none from Channalised prodelta. Table 5-10 lists the statistics of calculated vertical permeability values.

Comparison of the horizontal and vertical core plug permeabilities (Tables 5-4 and 5-10) reveals similar patterns. As for horizontal permeabilities, the means of vertical permeabilities are higher than the medians, for all lithofacies. The standard deviation and standard error of permeability measurements of vertical and horizontal plugs are relatively close values. All three lithofacies have high levels of heterogeneity, with $C_v$ values higher than 1 (Corbett and Jensen, 1992). The Tidal channel lithofacies show the same values of $C_v$ in both vertical and horizontal directions. The Tidal channel lithofacies have good reservoir properties (Martinius *et al.*, 1999). Figure 5-12 shows histograms of vertical permeability for three lithofacies. The vertical permeability data show similar patterns to those observed for the horizontal permeability data. The Delta

lobe lithofacies shows a narrow range of vertical permeability (except for two points). That could be explained as clean sand layers within the lithofacies where the bioturbation processes were not intensive (Martinius *et al.*, 2001). The wide range of vertical permeability values of the Basin floor lithofacies is discussed and tested analytically in this section. We suspect that the intensive bioturbation enhanced the vertical permeability.

Despite the fact that the vertical permeability is limited, it carries useful and helpful information for further evaluation of the permeability anisotropy of the Tilje Formation. The vertical permeability measurements are dispersed and, for the horizontal permeability, the medians are much higher than mean values.

**Table 5-10.** Statistics of the vertical core plug

| **No.** | 1 | 4 | 9 |
|---|---|---|---|
| **Lithofacies** | **Basin Floor** | **Delta lobe** | **Tidal channel** |
| **Min** | 0.1 | 0.2 | 0.1 |
| **Max** | 1030.0 | 2160.0 | 17500.0 |
| **Mean** | 246.6 | 217.8 | 2496.5 |
| **Median** | 48.6 | 5.4 | 557.0 |
| **SE** | 105.0 | 178.3 | 734.9 |
| **SD** | 348.4 | 617.5 | 4091.7 |
| **Cv** | 1.7 | 2.8 | 1.6 |

A comparison of vertical core plug permeability means and probe harmonic averages is given in Table 5-11. The core plug vertical permeability means are generally much higher than the harmonic averages of the probe data. An exception is Interval 5 from the Delta lobe lithofacies, which has the lowest $C_v$ value (Table 5-5) and was probably sampled from the homogeneous part of the lithofacies.

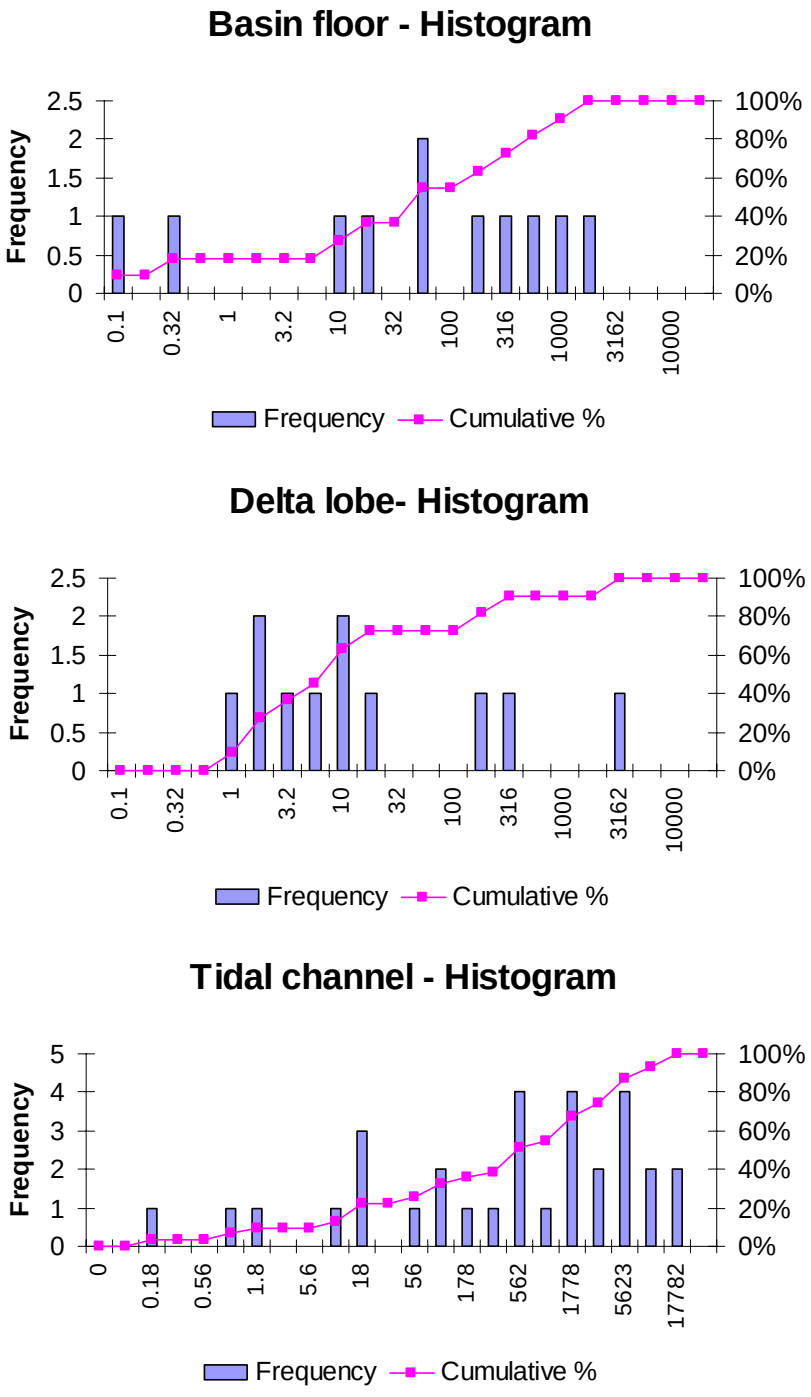


**Figure 5-12.** Histograms of the vertical core plug permeability for three lithofacies

The histogram plot of the vertical permeability of the Basin Floor facies (Figure 5-12) shows that the permeability values have a wide range (from 0.1 md to more than 1,000 md). A possible cause of this high degree of variation could be permeable microchannels created by bioturbation. A simple, three-layered model shows the concept (Figure 5-13). Channel A lies inside Layer 2. All parameters, length, thicknesses, and permeability used for this model are given in Table 5-12.

**Table 5-11.** Comparison table of core plug and probe means

| | | | Mean | |
|---|---|---|---|---|
| **No.** | **Lithofacies** | **Number** | **Probe** | **Core plug** |
| 4 | **Delta lobe** | **1** | 136.5 | 217.8 |
| | | **2** | 31.3 | |
| | | **3** | 98.5 | |
| | | **5** | 256.1 | |
| 9 | **Tidal channel** | **10** | 113.9 | 2496.5 |

The length of the channel A varies from 0.1 to 2.5 cm. For each change of the length of the channel, I calculated the vertical permeability of the system (Figure 5-14**)**. It was assumed that the direction of the flow is upwards, from the bottom to the top, and the flow influx per unit of length is constant. Meanwhile, from streamline simulation we know that all flow has a direction towards less resistance, otherwise, to high permeability.

The plot shows the changes of the vertical permeability with ratio (length of channel A to the length of layer 2). Small changes in the length increase the vertical permeability by orders of magnitude and alter the permeability ratio in the same manner.

Although this model has limitations, it shows an important effect: vertical permeability is strongly affected by minor imperfections in low permeability layers.

**Table 5-12.** Parameters of simple, three-layered model

| | Permeability, md | Thickness, cm | Length, cm |
|---|---|---|---|
| **Layer 1** | 1000 | 0.8 | 2.5 |
| **Layer 2** | 1 | 0.8 | 2.5 |
| **Layer 3** | 1000 | 0.8 | 2.5 |
| **Channel A** | 1000 | 0.8 | 0-2.5 |

***Conclusions***

The vertical core plug data are limited, which impairs evaluation of the impact of the lithology on permeability. However, based on the available data, some conclusions have been drawn. The difference between harmonic average and vertical permeability can occur for several reasons: sampling, volume of the sample, and depositional setting at the sampled interval. I experimentally proved that the vertical permeability can be enhanced by the bioturbation.

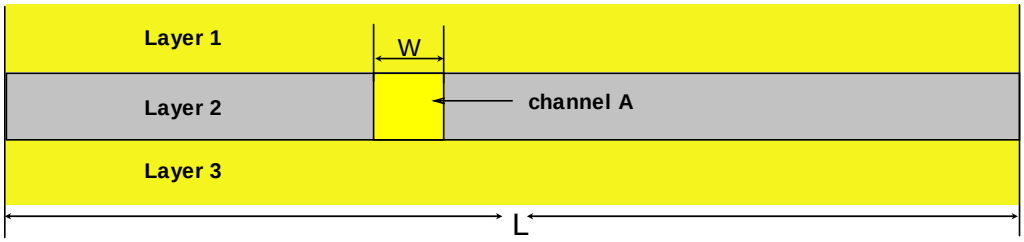


**Figure 5-13.** Simple three-layer model with highly permeable layer

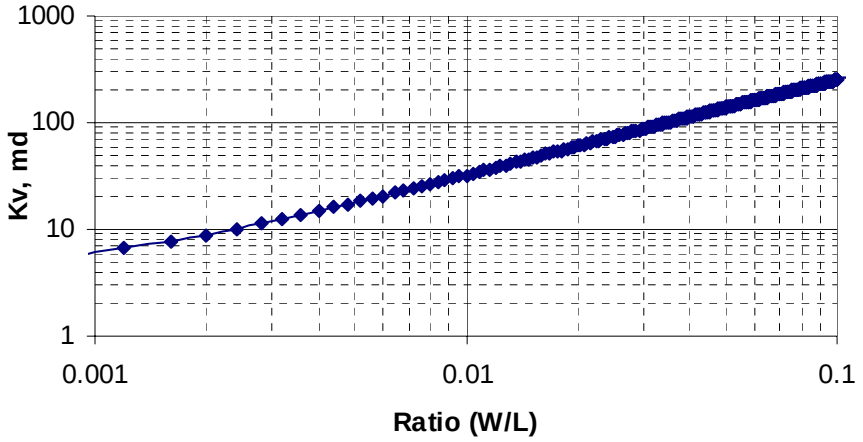


**Figure 5-14.** Small changes of the length increase the vertical permeability of the system

# CHAPTER VI
# PERMEABILITY ANISOTROPY EVALUATION

## 6.1 Introduction

The importance of permeability anisotropy in production and exploration of oil fields has been discussed in previous chapters. Heterogeneous reservoir rock can exhibit a wide range of permeability, thus affecting the permeability anisotropy. In this chapter, we turn to the problem of permeability anisotropy evaluation of the Tilje Formation.

## 6.2 Core plug permeability ratio

In Chapter V, horizontal and vertical core plug permeabilities were studied separately. Here, we assess the relationships between these two measurements. Figure 6-1 shows a plot of the vertical and horizontal core plug permeability. Data from six lithofacies are examined. The Transgressive and Inshore estuarine lithofacies are represented by only one and three vertical permeability core plugs, respectively. Only four core plugs pairs were sampled from the Prodelta heterolithic lithofacies and all the vertical plugs have permeability between 1 and 10 md. The remaining lithofacies exhibit a relatively linear pattern and, for the most part, the points fall into the isotropic range of permeability ratios (0.1 to 1).

Most of the time, the Tidal channel lithofacies has a permeability ratio of 1, which corresponds well to the homogeneity of the lithofacies (Figures 6-1 and 6-2). The Basin floor lithofacies has a similar pattern, but the vertical and horizontal permeabilities are lower. We must not forget about the intensive bioturbation that appears on some intervals of the lithofacies and can enhance the vertical permeability of the core plug. The Delta lobe lithofacies shows the lowest value of permeability ratio at 0.1 which could be caused by thick and more regularly spaced mudstone layers with variable thicknesses (Martinius *et al.,* 2001). However, the approximate spacing and thickness of the layers are not given.

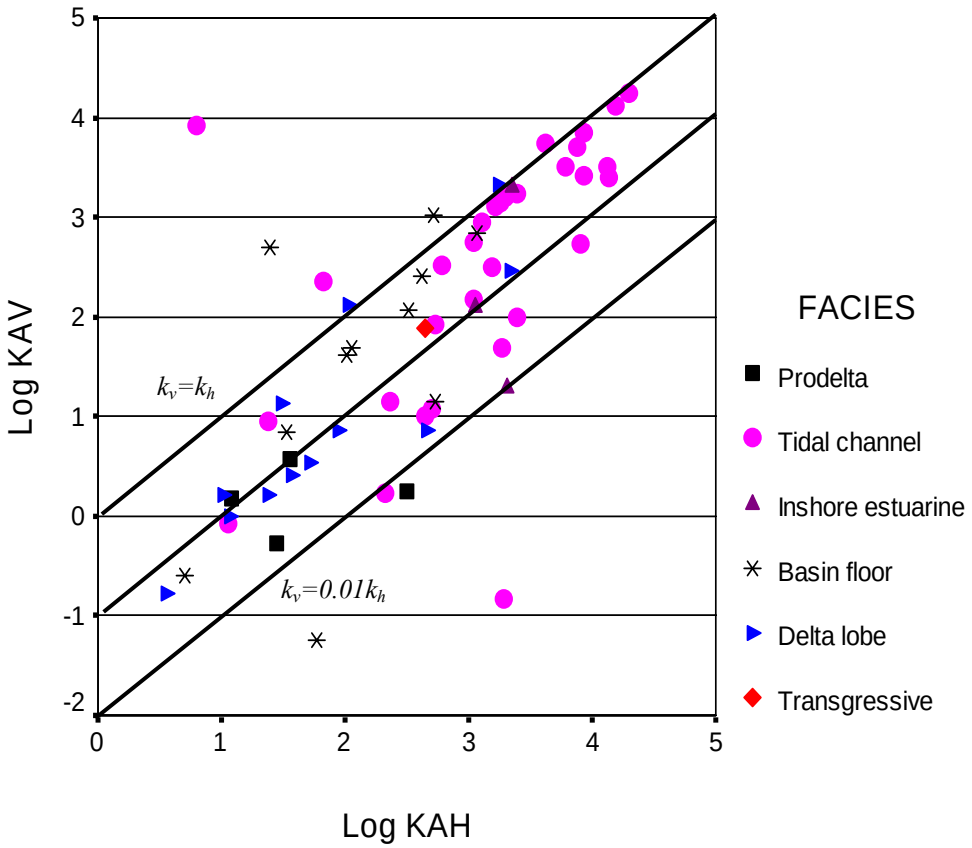


**Figure 6-1.** Core plug permeability ratio

The core plug permeability ratio depends on the vertical and horizontal permeabilities. Excluding a small number of samples from the set could lead to changes in heterogeneity measurement and permeability ratio. I calculated the $C_v$ values of horizontal and vertical permeability for three lithofacies given in Figure 6-2 using the Jacknife technique.

At the first stage, I eliminated one sample and calculated $C_v$. At the second stage, I excluded two samples and repeated the procedure, conducting several iterations for each stage. I evaluated the variability of $C_v$ after each stage statistically (Table 6-1). The $C_v$ values vary somewhat, but not enough to be unrepresentative of the heterogeneity of the reservoir lithofacies. For example, the Tidal channel $C_v$ of $k_h$ did not change from

1.3, and the $C_v$ of $k_v$ varied from 1.5 to 1.7 during the Stage 1 test. Considering the fact that the $C_v$ does not change significantly, we can conclude that the permeability ratio observed for the core plugs will not change considerably, so, we can rely on the Figure 6-1, which appears to present the actual core plug permeability ratios of the lithofacies.

**Table 6-1.** $C_v$ values after several iterations

| | | | | Cv | | |
|---|---|---|---|---|---|---|
| **Lithofacies** | **Number of iterations** | **Stages** | **$k_v/k_h$** | **Core** | **Min** | **Max** |
| Basin Floor | 11 | 1 | $k_h$ | **1.2** | 1.0 | 1.3 |
| | | | $k_v$ | **1.4** | 1.3 | 1.6 |
| | 30 | 2 | $k_h$ | **1.2** | 0.9 | 1.3 |
| | | | $k_v$ | **1.4** | 1.2 | 1.8 |
| Delta lobe | 12 | 1 | $k_h$ | **1.9** | 1.8 | 2.4 |
| | | | $k_v$ | **2.8** | 2.2 | 3.1 |
| | 40 | 2 | $k_h$ | **1.9** | 1.7 | 2.7 |
| | | | $k_v$ | **2.8** | 2.1 | 2.9 |
| Tidal channel | 31 | 1 | $k_h$ | **1.3** | 1.3 | 1.3 |
| | | | $k_v$ | **1.6** | 1.5 | 1.7 |
| | 100 | 2 | $k_h$ | **1.3** | 1.2 | 1.4 |
| | | | $k_v$ | **1.6** | 1.5 | 1.8 |

### 6.3 Minipermeameter (probe) permeability ratio

I assessed the permeability ratio for lithofacies sampled with the minipermeameter. Only the CDFs (Figure 4-1) of the minipermeameter measurements were available for this study. That is, the probe permeabilities were reported as the number of measurements falling within specific ranges, or ‘bin”.

To evaluate the permeability anisotropy, some additional data needed calculation. Using the CDFs, I assessed the arithmetic ($k_{aa}$) and harmonic ($k_{ha}$) averages (Table 6-2), assuming that $k_{aa}$ is equal to the horizontal permeability and $k_{ha}$ is the vertical permeability.

To calculate these quantities, I assumed a representative value for each bin. For the values in Table 6-2, I used the geometric average of each bin (Figure 6-3).

Meanwhile, to assess the robustness of these results, I made another calculation of $k_{aa}$ and $k_{ha}$, using the lower bin limit instead of the geometric average (Table 6-3). Figure 6-4 indicates only modest differences in $k_{aa}$ and $k_{ha}$ caused by the choice of value representing each bin. Table 6-2 and Table 6-3 list the results of the statistical analysis with calculated permeability ratios. The two tables indicate the same permeability ratios, $k_{ha}/k_{aa.}$

From the calculated permeability ratios from probe, I concluded that all lithofacies appear to have weak (from 0.1 to 1 md) anisotropy.

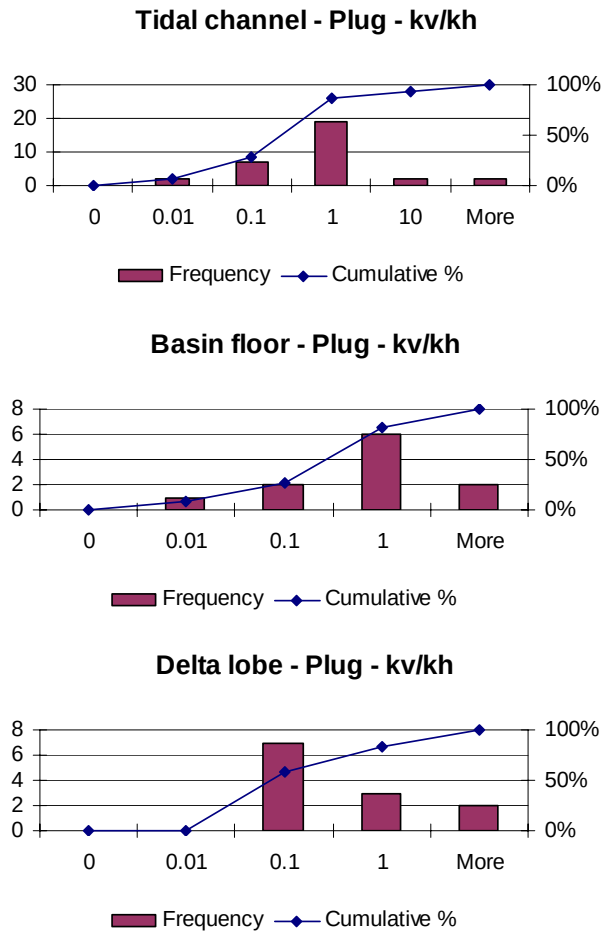


**Figure 6-2**. Histograms $k_v/k_h$ ratios of core plugs

To explore the influence of permeability and heterogeneity on the anisotropy, I used the $C_v$ and the ratio of the interquartile range ($IQR$) and median for the probe measurements.

**Table 6-2.** Permeability ratio calculated from geometric average

| No. | Lithofacies | Intervals | A. Mean ($k_{aa}$) | H. Mean ($k_{ha}$) | $k_{ha}/k_{aa}$ |
|---|---|---|---|---|---|
| 3 | **Prodelta heterolithic** | **6** | 279.9 | 47.6 | 0.2 |
| 4 | **Delta lobe** | **1** | 441.0 | 136.5 | 0.3 |
| | | **2** | 119.8 | 31.3 | 0.3 |
| | | **3** | 331.1 | 98.5 | 0.3 |
| | | **5** | 344.8 | 256.1 | 0.7 |
| 9 | **Tidal channel** | **10** | 225.9 | 113.9 | 0.5 |

**Table 6-3.** Permeability ratio calculated from the lower bin limit

| No. | Lithofacies | Intervals | A. Mean ($k_{aa}$) | H. Mean ($k_{ha}$) | $k_{ha}/k_{aa}$ |
|---|---|---|---|---|---|
| 3 | **Prodelta heterolithic** | **6** | 209.9 | 35.7 | 0.2 |
| 4 | **Delta lobe** | **1** | 330.7 | 102.3 | 0.3 |
| | | **2** | 89.8 | 23.5 | 0.3 |
| | | **3** | 248.3 | 73.9 | 0.3 |
| | | **5** | 258.5 | 192.0 | 0.7 |
| 9 | **Tidal channel** | **10** | 169.4 | 85.4 | 0.5 |

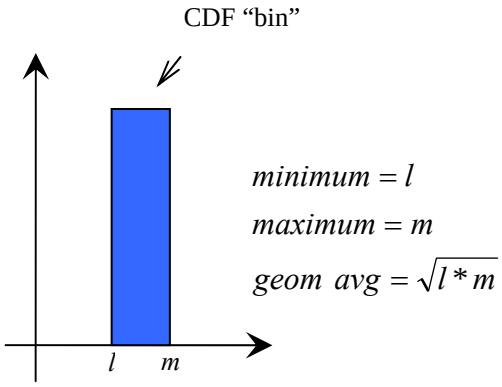


**Figure 6-3.** Example of a bin

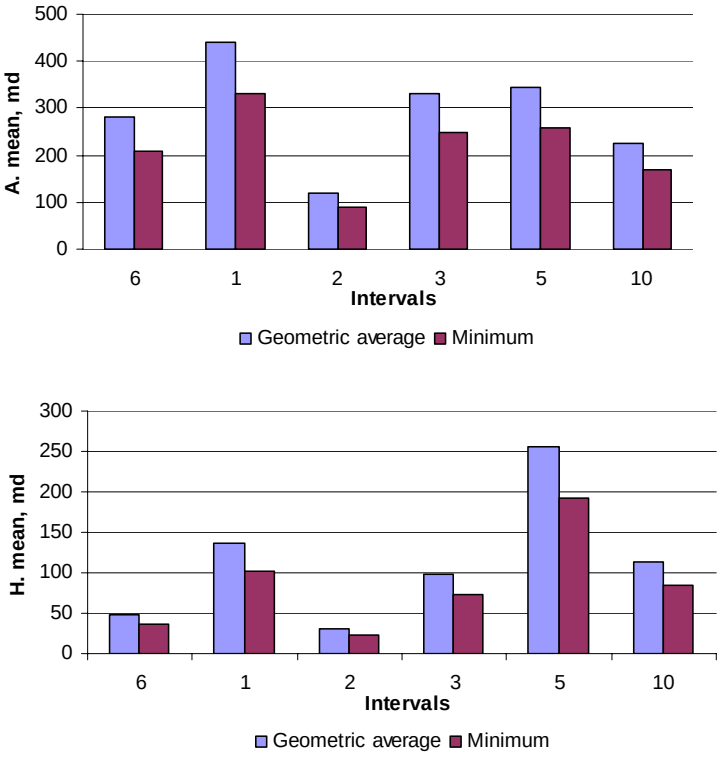


**Figure 6-4**. Permeability means show almost the same ranges, whether using the geometric average of the upper and lower values for each bin or just using the minimum value for each bin

Plots of dimensionless *IQR/Median* (=$C_v'$) versus the median and $C_v$ versus the arithmetic mean (Figure 6-5) show the relationship of anisotropy of a sample with heterogeneity. Generally speaking, the greater $C_v'$ or $C_v$, the more anisotropy we observe. The top plot (Figure 6-5) shows a weaker relationship than the bottom does because of the effect of the high permeability values on $C_v$. The position of Intervals 2, 3, 5, and 10 remains the same on both plots, indicating that they represent more isotropic reservoir rock. As expected, Interval 5 of the Delta lobe lithofacies represents the most isotropic reservoir rock sample, having the highest median and arithmetic mean; it presents a relatively homogeneous part of the lithofacies. $C_v'$ and $C_v$ for the Prodelta heterolithic lithofacies (Interval 6) are increased from one measurement to another, caused by the highpermeability values affecting $C_v$. Interval 1 of the Delta lobe lithofacies shows the same heterogeneity, but has a lower median, because of a few high-permeability points observed on the minipermeameter probe histogram (Fig 4-1).

The general trends observed in Figure 6-5 are as expected. If heterogeneity increases, the anisotropy of the sample also increases. This is generally true for all permeability measurements. Relationships between heterogeneity and anisotropy were previously discussed in the Chapter V.

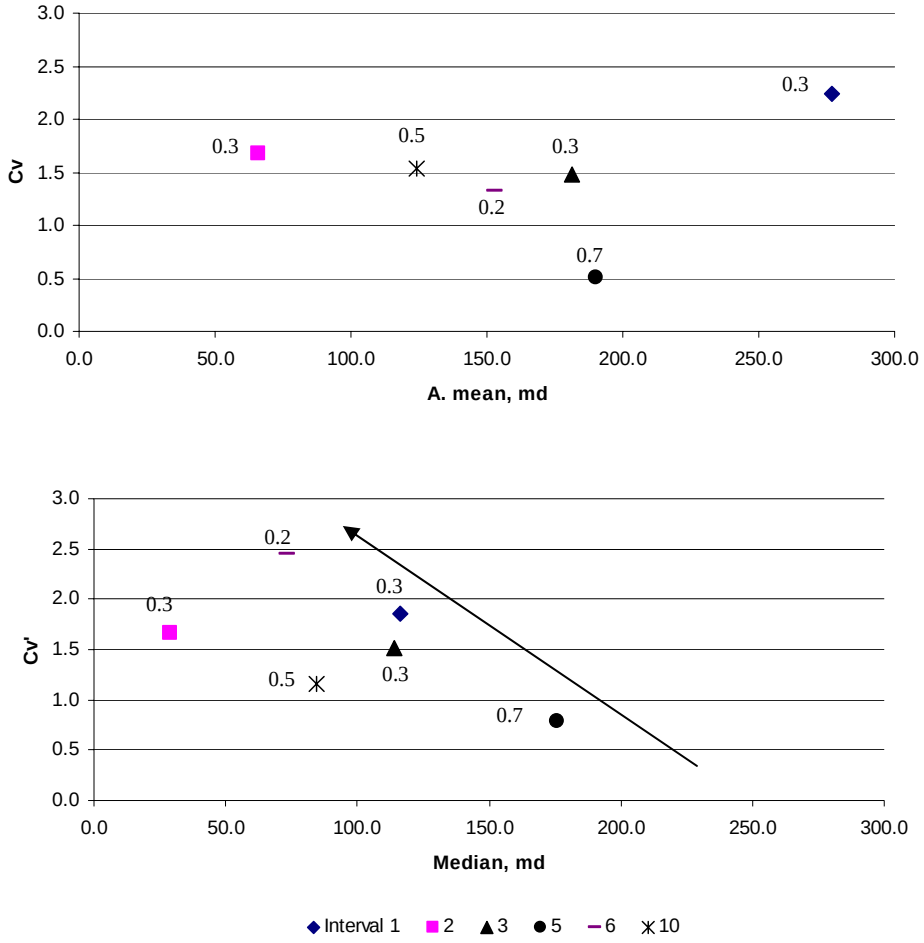


**Figure 6-5.** Permeability anisotropy ($k_{ha}/k_{aa}$) increases with heterogeneity of sample

## 6.4 Comparison of core plug and probe permeability ratios

Core plug and probe permeability measurements allow permeability anisotropy evaluation. Comparison of these two data is necessary for anisotropy evaluation of the lithofacies at different scales.

Here, only two lithofacies can be compared as only the Delta lobe and the Tidal channel probe and core plug measurements are available. The probe-permeability ratios are in the same range as the core plug permeability ratios.

According to the permeability anisotropy from probe and core plug data (Figure 6-2 and Table 6-3), the Delta lobe and Tidal channel lithofacies are isotropic.

**6.5 Observations**

Permeability anisotropy evaluation is an important tool to assess the reservoir properties of the formation for the purpose of reservoir modeling. The core plug and minipermeameter measurements can capture the heterogeneity and can be used to judge the permeability anisotropy for these particular lithofacies. Although in this case the data are limited for this type of analysis, this study did not reveal a high degree of permeability anisotropy for the lithofacies from the Tilje Formation.

This result contradicts the results obtained by Martinius *et al.,* (1999). The study conducted by Martinius *et al.* (1999, Table 1b) finds strong anisotropy for some lithofacies of the Tilje Formation. The difference between the results of these authors' and mine appear to be caused by the combination of the model they used and the core plug they chose for comparison.

Their approach (Martinius *et al.,* 1999) consists of several stages; starting with the mathematical model of sub-meter bedding architecture and concluding with the evaluation of an upscaled geostatistical model at the reservoir-scale. The anisotropy value of the model is 0.006 for the heterolithic and delta front lithofacies (Figure 6-6). The bold line on the plot shows the permeability anisotropy of their model and the points on the plot represent the core plug permeability anisotropy values measured for these lithofacies. Martinius *et al.* (1999) compared the permeability ratio of the model with the permeability ratios from selected core plugs and claimed to have good agreement. Clearly, their favorable comparison must be based on only a few core plug pairs. More core plug pairs were used for this study and Figure 6-6 shows that the majority of the points fall within the isotropic range.

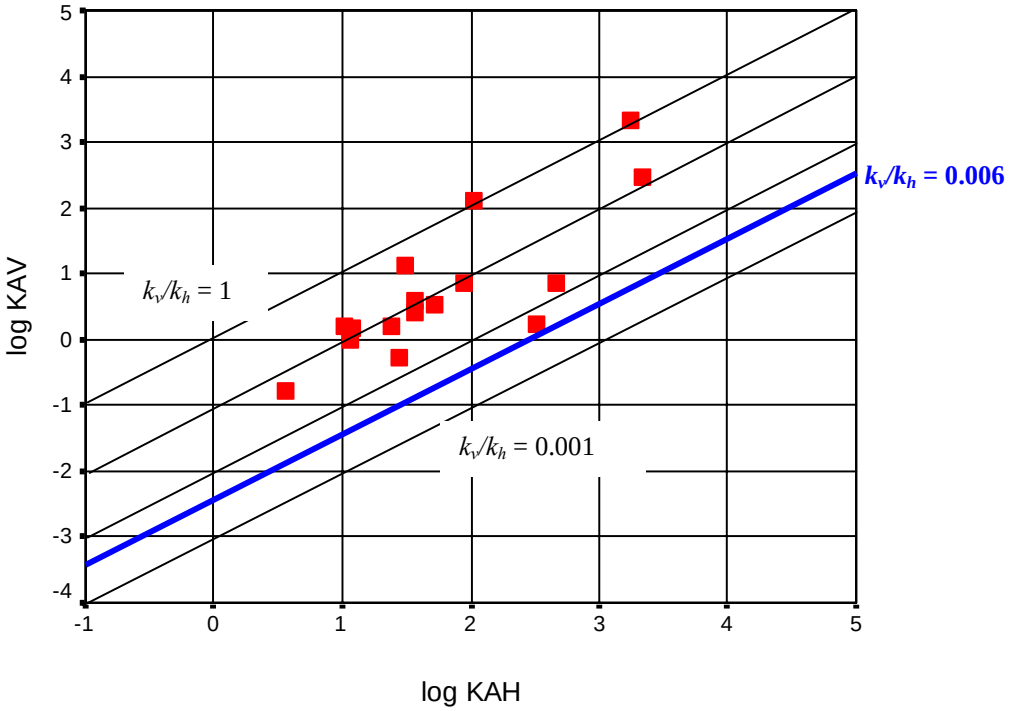


**Figure 6-6**. Comparison plot of the core plug permeability of the Prodelta heterolithic and Delta front lithofacies examined for this study and result of the Martinius *et al.,* (1999) for the same lithofacies

Another reason for the difference between Martinius *et al.*'s (1999) results and mine could be a matter of assumptions they used for the mathematical model. They modeled a cube of wavy bedding (Martinius *et al.,* Figure 8, 1999), used to generate the facies-scale model, and it shows continuous mudstone layers. However, there are some possibilities that low permeability layers might not be laterally extensive or otherwise contain imperfections (holes). This scenario was not considered by Martinius *et al.,* (1999). A small hole in the mudstone layers could substantially reduce the anisotropy, as shown in the three-layer model of Section 5.8.

Thus, the much stronger anisotropy predicted by Martinius *et al.,* (1999) suggests a pessimistic interpretation of the data. Perhaps, further information available for them

(e.g., more details of the probe permeability measurements and core from other wells) justifies this approach.

# CHAPTER VII
# CONCLUSIONS

Core plug and minipermeameter permeability data were used for this research. The following conclusions result:

1. Although the volume of core plug and minipermeameter sample is different, the lithology and depositional settings influenced the minipermeameter measurements.
2. Different scales of sample measurements capture the heterogeneity of the reservoir rock, as is supported by statistically evaluated heterogeneity of the probe and core plug
3. The difference between harmonic average of the probe data and vertical core plug permeability measurements using different methods reflect sampling, volume of the sample, and depositional setting at the sampled interval.
4. Experiments suggest that vertical permeability can be enhanced by bioturbation.
5. Although the data are limited for this type of analysis, this study did not reveal a high degree of anisotropy for the lithofacies from the Tilje Formation. The assumption of isotropic reservoir rock, with high horizontal and vertical permeability, for lithofacies Channalised delta-front lobe and Inshore estuarine agrees with available geological references (Martinius *et al.,* 1999 and 2001).
6. The results of the permeability anisotropy evaluation applied for analyzing of large formation-scale is uncertain. Permeability anisotropy of the lithofacies of the Tilje Formation varies in a certain range. Reservoir simulation is required to assess permeability anisotropy of lithofacies applicable at the formation-scale.
7. This research did not reveal strong anisotropy. The difference between these results and those of Martinius *et al*. (1999) is probably due to an explicit permeability model used by Martinius and the others from Statiol.

## REFERENCES CITED

Ayan, C., N. Colley, G. Cowan, E. Ezekwe, M. Wannell, P. Goode, F. Halford, J. Joseph, A. Mongini and J. Pop, 1994, Measuring permeability anisotropy: The latest approach: Oilfield Review, v. 6, no. 4, p. 24-35.

Begg, S.H. and P.R. King, 1985, Modelling the effects of shales on reservoir performance: Calculation of effective vertical permeability: The 1985 Society of Petroleum Engineers Reservoir Simulation Symposium, Dallas, Texas, 10-13 February, SPE Paper 13529, 15 p.

Corbett, P. and J.L. Jensen, 1992, Variation of reservoir statistics according to sample spacing and measurment type for some intervals in the lower Brent group: The Log Analyst, v. 33, no. 1, p. 22-41.

Cowan, G. and J. Bradney, 1997, Regional diagenetic controls on reservoir properties in the millom accumulation: Implications for field development, *in* N.S. Meadodws, S.P. Truebood, M. Hardman, and G. Cowan, eds., Petroleum geology of the Irish Sea and adjacent area: Geological Society (London) Special Publication 124, p. 382-386.

Green, W.D. and G.P. Willhite, 1998, Enhanced oil recovery textbook: The Society of Petroleum Engineers Textbook Series 6, p 235.

Hurst, A. and K. J. Rosvoll, 1991, Permeability variations in sandstones and their relationship to sedimentary structures, *in* L.W Lake, H.B. Carroll Jr and T.C. Wesson, eds., Reservoir Characterization II: Academic Press Inc., p. 166-196.

Jensen, J.L., L.W. Lake, P.W.M. Corbett, and D.J. Goggin, 2003, Statistics for petroleum engineers and geoscientists, 2nd Edition: New York, Elsevier, 338 p.

Kasap, E., 2001, Estimating ratio for conductive and nonconductive shales and mudstones: The 2001 Society of Petroleum Engineers Western Regional Meeting, California, 26-30 March, SPE Paper 68782, 12 p.

Lake, W.L., 1988, The origins of anisotropy: Journal of Petroleum Engineering, v. 6 no. 4, p. 395-398.

Martinius, A.W., K. Inge, A. Nass, G. Helgesen, J. M. Kjerefjord and D. A. Leith, 2001, Sedimentology of the heterolithic and tide-dominated Tilje Formation (Early Jurassic), Halten Terrace, offshore Mid-Norway, *in* O.J. Matrinsen and T. Dreyer, eds., Sedimentary environments offshore Norway – Palaeozoic to recent: Norwegian Petroleum Society Special Publication 10, p. 103-144.

Martinius, A. W., P.S. Ringrose, A, Nass and R. Wen, 1999, Multi-scale characterization and modeling of heterolithic tidal systems, offshore mid-Norway: Gulf Coast Section SEPM Foundation Research Conference on Advance Reservoir Characterization for the Twenty-first Century, Houston, Texas, 5-8 December, 21 p.

Morton, K., S. Thomas, P. Corbett, and D. Davies, 2002, Detailed analysis of probe permeameter and interval pressure transient tests permeability measurements in a heterogeneous reservoir: Petroleum Geosience, v. 8, no. 3, p. 209-216.

Neave, H.R., 1978, Statistics tables for mathematicians, engineers, economists and the behavioural and management science: London, George Allen & Unwin, 88 p.

Neave, H.R., and P.L. Worthington, 1988, Distribution-free test: London, Unwin Hyman, 430 p.

Peffer, J., A. O'Callaghan, and J. Pop, 1997, *In-situ* determination of permeability anisotropy and its vertical distribution – A case study: The 1997 Society of Petroleum Engineers Annual Technical Conference and Exhibition, San Antonio, Texas, 5-8 October, SPE paper 38942, 10 p.

Whitley P.K., 1992, The Geology of Heidrun: A giant oil and gas filed on the mid-Norwegian shelf, *in* M.T. Halbouty ed., Giant Oil Fields of the Decade 1978-1988: AAPG Memoir 54, p. 383-406.

Willhite G.P., 1986, Waterflooding: The Society of Petroleum Engineers Textbook Series 3, 326 p.

# APPENDIX A

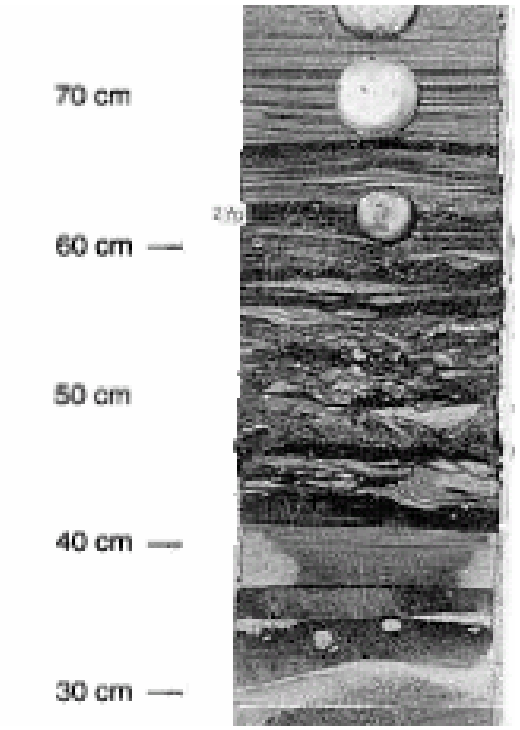


**Basin Floor lithofacies**

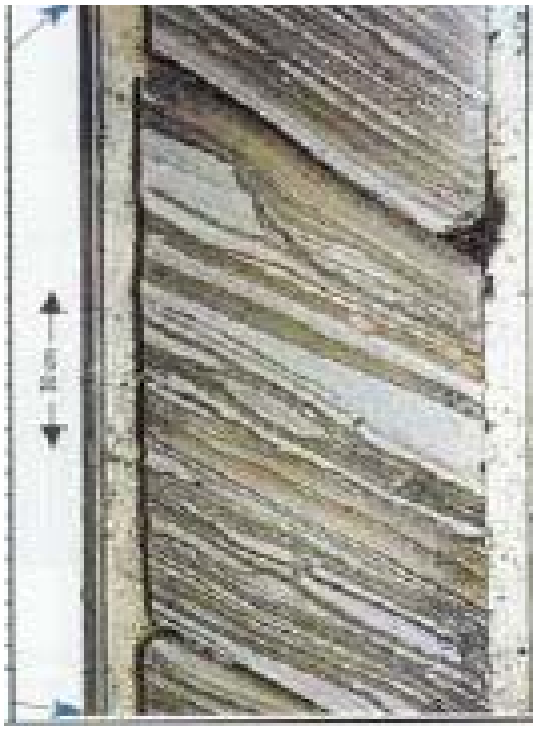

**Prodelta heterolithic lithofacies**


**Delta-front lobe lithofacies**

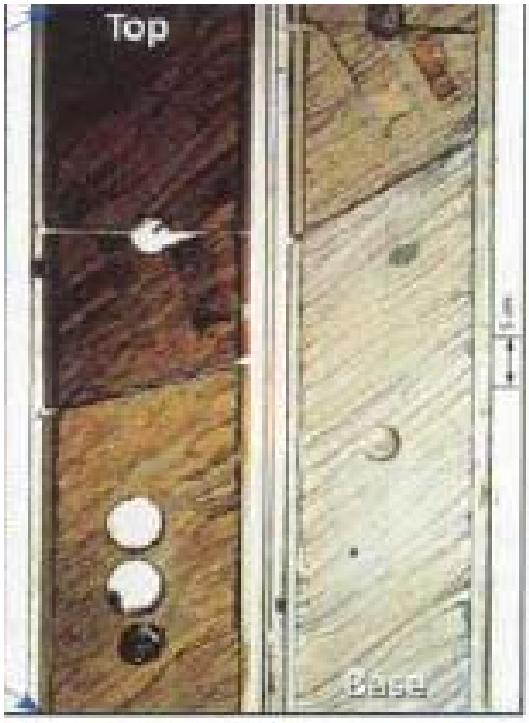


**Channalised delta-front lobe**

**Inshore estuarine**

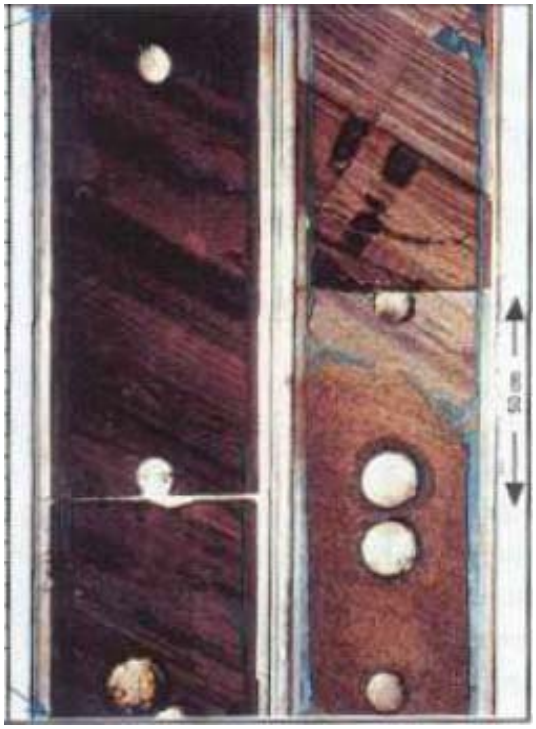

**Tidal channel lithofacies**

# VITA

**Kanan R. Aliyev**
14 A. Manafov St., Apt#36, Baku, Azerbaijan, 370060
Tel: (+994 12) 23 7778 Email: aliyevker@yahoo.co.nz Fax: (734) 549-5985
(+994 50) 351 7778

**Education Background**
**Texas A&M University, Petroleum Engineering Department** -September - 2002 – August 2004 –M.S. in petroleum engineering

**Baku State University, Faculty of Geology, Department of Exploration Mineral Resources** - September 1999 – July 2001 - M.S. in geology

**Baku State University, Faculty of Geology, Department of Exploration Mineral Resources** - September 1995 – July 1999 - B.S. in geology

**Work Experience**
**BP Caspian Sea Exploration** – June 2002 – August 2002 - Geoscientist Internship- Amu-Dar'ya basin study – basin analysis, reservoir performance, reserves estimation.

**SALYANOIL Co. Ltd.** [Production Share Company of SOCAR (Azerbaijan), Frontera (USA), Amerada HESS (UK)]. – June 2001 – August 2001 - Junior geologist - Well log interpretation and geological support in a petrophysical team.

**SALYANOIL Co. Ltd**. [Production Share Company of SOCAR (Azerbaijan), Frontera (USA), Amerada HESS (UK)]. – March 2001 – June 2001 - Geologist-Trainee - Preparing LAS, ASCII, SMT files for a subsurface mapping team.

**Denizneftgaslayihe - State Scientific Research and Design Institute, SOCAR** (State Oil Company of Azerbaijan Republic) – October 1998 – March 2001 - Geologist - Preparing projects for future directions of exploration (team base work)

**Denizneftgaslayihe** - **State Scientific Research and Design Institute, SOCAR** (State Oil Company of Azerbaijan Republic) – April 1998 – October 1998 - Geo-technician - Gathering information about exploration wells from various offshore fields.

**Scholarships**
**American Geological Institute Non-Degree Scholarship** – August 2001 – May 2002, Texas A&M University, Department of Geology and Geophysics

**BP Scholarship for Petroleum Engineers and Geoscientists** – September 2002 – May 2004, Texas A&M University, Department of Petroleum Engineering